



## **A57: Investigate Detect & Avoid (DAA) Track Classification & Filtering Final Report**

December 6, 2024

## **NOTICE**

This document is disseminated under the sponsorship of the U.S. Department of Transportation in the interest of information exchange. The U.S. Government assumes no liability for the contents or use thereof. The U.S. Government does not endorse products or manufacturers. Trade or manufacturers' names appear herein solely because they are considered essential to the objective of this report. The findings and conclusions in this report are those of the author(s) and do not necessarily represent the views of the funding agency. This document does not constitute FAA policy. Consult the FAA sponsoring organization listed on the Technical Documentation page as to its use.

## **LEGAL DISCLAIMER**

The information provided herein may include content supplied by third parties. Although the data and information contained herein has been produced or processed from sources believed to be reliable, the Federal Aviation Administration makes no warranty, expressed or implied, regarding the accuracy, adequacy, completeness, legality, reliability or usefulness of any information, conclusions or recommendations provided herein. Distribution of the information contained herein does not constitute an endorsement or warranty of the data or information provided herein by the Federal Aviation Administration or the U.S. Department of Transportation. Neither the Federal Aviation Administration nor the U.S. Department of Transportation shall be held liable for any improper or incorrect use of the information contained herein and assumes no responsibility for anyone's use of the information. The Federal Aviation Administration and U.S. Department of Transportation shall not be liable for any claim for any loss, harm, or other damages arising from access to or use of data or information, including without limitation any direct, indirect, incidental, exemplary, special or consequential damages, even if advised of the possibility of such damages. The Federal Aviation Administration shall not be liable to anyone for any decision made or action taken, or not taken, in reliance on the information contained herein.

**TECHNICAL REPORT DOCUMENTATION PAGE**

<b>1. Report No.</b> A11.L.UAS.100	<b>2. Government Accession No.</b>	<b>3. Recipient's Catalog No.</b>
<b>4. Title and Subtitle</b> A57 Investigate Detect and Avoid Track Classification and Filtering Task 3 Report		<b>5. Report Date</b> December 5, 2024
<b>7. Author(s)</b> Matthew McCrink, Ph.D., <a href="https://orcid.org/0000-0003-2212-2132">https://orcid.org/0000-0003-2212-2132</a> Dhuree Seth, Ph.D., <a href="https://orcid.org/0000-0001-7759-6453">https://orcid.org/0000-0001-7759-6453</a> Bouteina Driouche, Ph.D., <a href="https://orcid.org/0000-0001-7034-0930">https://orcid.org/0000-0001-7034-0930</a> Bryan C. Farrell, <a href="https://orcid.org/0000-0003-1674-9043">https://orcid.org/0000-0003-1674-9043</a> Kyle B. Ryker Seunghan Lee, Ph.D. Asishana Ajayi Aryslan Malik, Ph.D. Houbing Song, Ph.D. Morad Nazari, Ph.D. Richard J. Prazenica, Ph.D. Troy Henderson, Ph.D. Tyler Spence, Ph.D. Richard Stansbury, Ph.D. Jichul Kim, Ph.D. Brady Swann		<b>6. Performing Organization Code</b>  <b>8. Performing Organization Report No.</b>
<b>9. Performing Organization Name and Address</b> The Ohio State University Department of Mechanical and Aerospace Engineering Aerospace Research Center 2300 W Case Rd Columbus OH 43235		<b>10. Work Unit No.</b>
<b>12. Sponsoring Agency Name and Address</b> Federal Aviation Administration		<b>11. Contract or Grant No.</b>
<b>15. Supplementary Notes</b>		<b>13. Type of Report and Period Covered</b> Final report draft
		<b>14. Sponsoring Agency Code</b> 5401

**16. Abstract**

This report summarizes the primary sources of error in ground and airborne sensors leading to false or misleading tracks being presented to the operator of autonomous Uncrewed Aircraft Systems (UAS). The primary focus of this research is to demonstrate risk modelling strategies to understand the impact of false information on detect and avoid systems currently being developed and deployed for UAS. This report documents the proposed encounter scenarios investigated using advanced simulations to assess the impact of changing clutter flux density.

**17. Key Words**

sUAS, clutter, radar, detect and avoid, false tracks, risk identification

**18. Distribution Statement**

No restrictions.

**19. Security Classification (of this report)**

Unclassified

**20. Security Classification (of this page)**

Unclassified

**21. No. of Pages**

85

**22. Price**

N/A

Form DOT F 1700.7 (8-72)

Reproduction of completed page authorized

## TABLE OF CONTENTS

NOTICE.....	I
LEGAL DISCLAIMER.....	II
TECHNICAL REPORT DOCUMENTATION PAGE.....	III
TABLE OF FIGURES.....	VIII
TABLE OF TABLES.....	X
TABLE OF ACRONYMS.....	XI
EXECUTIVE SUMMARY.....	XII
1 INTRODUCTION & BACKGROUND.....	1
1.1 Final Report Overview.....	1
1.2 Risk Metrics and Encounter Datasets.....	1
1.3 Simulation Environment and Algorithms.....	1
1.4 Clutter Modeling and Impact Analysis.....	1
1.5 Experimental Data Collection.....	1
1.6 Operational Suitability and Safety.....	1
1.7 Pilot Surveys.....	2
1.8 Risk Metrics.....	2
1.9 Encounter Sets.....	2
1.9.1 Glendale Encounter Set.....	2
1.9.2 MIT Terminal Area Encounter Set.....	3
1.9.3 Cooperative Surveillance Parameters.....	4
1.10 Fast-Time Simulation Environment.....	4
1.10.1 Enroute Encounters.....	4
1.10.2 Terminal Operations.....	5
1.11 Clutter Metrics.....	6
1.11.1 Types of Clutter in the Air Picture and Their Operational Impact.....	6
1.11.2 Clutter Flux.....	7
1.11.3 Clutter Flux Density.....	7
1.11.4 Clutter Clustering.....	8
1.11.5 Navigable Fraction.....	9
1.11.6 Clutter Risk Ratio Delta.....	9
1.11.7 Clutter Probability of Detection.....	9
1.11.8 Missed Object and False Track Flux.....	10

1.11.9	Missed Relevant Track Flux .....	11
1.11.10	Probability of Retained Clutter .....	11
1.11.11	Summary .....	12
2	SENSOR DATA COLLECTION AND ANALYSIS .....	12
2.1	Introduction .....	12
2.2	Iris Automation’s Casia-G Sensor.....	12
2.2.1	Methodology and Safety Measures.....	12
2.2.2	Conclusions.....	14
2.3	EO/IR Modeling and Analysis Efforts.....	15
2.3.1	Approaches Used .....	15
2.3.2	Case 1: High – Max .....	15
2.3.3	Case 2: Medium .....	20
2.3.4	Case 3: Low .....	24
2.4	Data Modeling and Synthetic Dataset Generation .....	29
3	ENROUTE MODELING AND SIMULATION RESULTS .....	35
3.1	Simulation Setup .....	35
3.2	Ground Based Radar Results.....	35
3.2.1	Safety Analysis: Nominally Alerting Encounters.....	35
3.2.2	Safety Analysis: 10K Nominally Alerting Encounters.....	37
3.2.3	Non-alerting encounters, Full Clutter .....	38
3.2.4	Delayed clutter .....	39
3.2.5	AGT Transition.....	41
3.2.6	Operational Suitability Analysis.....	41
3.3	EO/IR results .....	42
3.3.1	MSU Variable Density Clutter.....	42
3.3.2	Operational Suitability Analysis.....	44
3.3.3	MSU Clutter Data: Safety Analysis.....	44
4	TERMINAL MODELING AND SIMULATION RESULTS .....	45
4.1	Simulation Setup .....	45
4.2	Ground-Based EO/IR Results .....	46
5	CLUTTER IMPACT ON OPERATIONS .....	55
5.1	Overview .....	55
5.2	Description of Systems.....	56

5.3	Field Tests .....	56
5.4	Surveys .....	57
5.5	Results .....	57
5.6	Recommendations .....	58
6	CONCLUSIONS .....	59
6.1	Enroute Encounters .....	60
6.2	Terminal Encounters .....	61
6.3	Clutter Impact on Operations .....	62
6.4	Future Research Needs.....	62
7	REFERENCES .....	64

## TABLE OF FIGURES

Figure 1. Glendale alerting encounter set. ....	3
Figure 2. Horizontal and Vertical Separation: ACAS sXu Mitigation (closed-loop) vs Unmitigated (open-loop).....	5
Figure 3. Raspet Detect and Avoid System. ....	6
Figure 4. IRIS Automation’s Casia G. Sensor (left), Judy power supply system (center) and SIERRA wireless router (right). ....	12
Figure 5. South farm data collection location.....	13
Figure 6. Rice Hall data collection location.....	14
Figure 7. Clutter modeling using distributed fitting. ....	15
Figure 8. Scatter Plots among latitude, longitude, and altitude in a high density.....	16
Figure 9. Histograms of (a) Latitude, (b) Longitude, and (c) Altitude in a high density.....	17
Figure 10. Empirical CDFs – latitude, longitude, and altitude in a high density.....	18
Figure 11. Real EO/IR clutter vs Simulated EO/IR clutter in a high-density.....	19
Figure 12. Scatter plots in a medium clutter density environment. ....	21
Figure 13. Histograms of latitude, longitude, and altitude in a medium clutter density environment. ....	22
Figure 14. The cumulative density function of latitude, longitude, and altitude in a medium clutter density environment.....	23
Figure 15. Real EO/IR clutter vs Simulated EO/IR clutter in a medium clutter density environment. ....	24
Figure 16. Scatter plots in low clutter density environment. ....	25
Figure 17. Histograms of latitude, longitude, and altitude in a low clutter density environment. ....	26
Figure 18. The cumulative density function of latitude, longitude, and altitude in a low clutter density environment.....	27
Figure 19. Real EO/IR clutter vs Simulated EO/IR clutter in a medium clutter density environment. ....	28
Figure 20. Altitude distribution of single clutter dataset, in feet. ....	31
Figure 21. Velocity in x-direction (horizontal) for clutter data, in feet per second.....	31
Figure 22. Velocity in y-direction (horizontal) for clutter data, in feet per second.....	31
Figure 23. Velocity in z-direction (vertical) for clutter data, in feet per second. ....	32
Figure 24. Resulting wider area of clutter data, with 30-minute length. ....	33
Figure 25. Various distribution comparisons of field data (left) and simulated data (right). ....	35
Figure 26. Histogram showing differences in LoWC with and without Clutter. Chart on the right indicates that LoWC is due to early alerting and diverting of the ownship. When a delay to alert only when in proximity to the intruder (figure on the right), the LoWC rates better align with the intruder-only data sets.....	37
Figure 27. Modification to mask clutter until after intruder triggers alert.....	40
Figure 28. Total alert duration and number of split alerts per encounter. ....	42
Figure 29. Number of reversals per encounter with varying levels of clutter. ....	42
Figure 30. Low density clutter.....	43
Figure 31. Medium density clutter.....	43
Figure 32. High density clutter. In these charts, ownship trajectories are shown in blue, intruders in red, and clutter in green. ....	43

Figure 33. Number of split alerts and alert durations per encounter for model-based clutter. ....	44
Figure 34. Approach corridor definition for lateral boundaries (top), and vertical boundaries (bottom).....	46
Figure 35. Subset of ownship trajectories meeting the missed approach threshold requirements, shown in pink. Blue tracks do not intersect the approach corridor and were discarded. ....	46
Figure 36. Low-rate clutter raw (left), with 3 second filter (middle) and 5 second filter (right)..	47
Figure 37. Medium-rate raw (left), with 3 second filter (middle) and 5 second filter (right).....	47
Figure 38. Medium-high rate raw (left), with 3 second filter (middle) and 5 second filter (right). .....	48
Figure 39. High-rate raw (left), with 3 second filter (middle) and 5 second filter (right). ....	48
Figure 40. Description of symbols used in the trajectory graphs shown below. ....	50
Figure 41. Flight trajectory in chronological order (left to right) of ownship-only case.....	50
Figure 41. Flight trajectory in chronological order (left to right) of ownship + intruder case. ....	51
Figure 42. Flight trajectory in chronological order (left to right) of ownship + clutter (Low) case. .....	51
Figure 43. Flight trajectory in chronological order (left to right) of ownship + intruder + clutter (Low) case.....	52
Figure 44. Flight trajectory of ownship + intruder + clutter for Low/Medium/Medium High/High (left to right) cases. ....	52
Figure 45. Basic schematic of the primary and the isolated secondary autopilot onboard the large UAS.....	56
Figure 46. Word cloud of most prominent words, visualized by larger fonts, used by the research team when qualitatively evaluating the DAA system’s clutter.....	58

## TABLE OF TABLES

Table 1. Analysis Metrics. ....	2
Table 2. Ownship and Intruder Vehicle Surveillance Parameters. ....	4
Table 3. Surveillance Sensor Uncertainty. ....	4
Table 4. Correlation between latitude, longitude, and altitude in a high clutter density environment. ....	15
Table 5. Correlation between latitude, longitude, and altitude in a medium clutter density environment. ....	20
Table 6. Correlation between latitude, longitude, and altitude in a low clutter density environment. ....	24
Table 7. Analysis for varying levels of clutter. (Note, reduction in safety statistics are due to likely simulation bias as noted in 3.2.1). ....	36
Table 8. LoWC changes based on levels of clutter.(Note, reduction in safety statistics are due to likely simulation bias as noted in 3.2.1) ....	36
Table 9. Analysis including treatment of clutter as ‘Real’ tracks. (Note, reduction in safety statistics are due to likely simulation bias as noted in 3.2.1). ....	38
Table 10. Analysis including treatment of clutter as ‘Real’ tracks in percentage. (Note, reduction in safety statistics are due to likely simulation bias as noted in 3.2.1) ....	38
Table 11. Analysis using 65K non-alerting encounters. ....	39
Table 12. Results following simulation modification where clutter is hidden in the simulation until after there is an alert on the intruder aircraft. ....	40
Table 13. Statistics using ADS-B vs AGT DAA interface for intruder. ....	41
Table 14. Summary of encounters using EO/IR sensor data with varying clutter characteristics. OpVal refers to previously published data from MIT for the same encounters, Results are from simulations conducted in this work, and the Target are the ASTM LoWC ratio and NMAC risk ratios. (Note, reduction in safety statistics are due to likely simulation bias as noted in 3.2.1) ..	44
Table 15. Analysis using alerting encounters with model-based clutter data. (Note, reduction in safety statistics are due to likely simulation bias as noted in 3.2.1) ....	45
Table 16. Clutter-flux densities tested in the terminal environment in false tracks/(nm <sup>2</sup> -hr).....	47
Table 17. Number of samples and tracks for different levels of clutter on filtering options. ....	48
Table 18. Average of alerts per flight and average of alerts per minute for 3-second filtered clutter data. ....	53
Table 19. Average of alerts per flight and average of alerts per minute for 5-second filtered clutter data. ....	53
Table 20. Missed approach percentage, LoWC, NMAC, and reversals for low-clutter case (5s filter). ....	54
Table 21. Missed approach percentage, LoWC, NMAC, and reversals for Med-clutter case (5s filter). ....	55
Table 22. Missed approach percentage, LoWC, NMAC, and reversals for Med-High-clutter case (5s filter). ....	55
Table 23. Missed approach percentage, LoWC, NMAC, and reversals for High-clutter case (5s filter). ....	55

## TABLE OF ACRONYMS

AGT	Absolute Geodetic Track
ART	Avoidance Required Threshold
ATC	Air Traffic Control
ADS-B	Automatic Dependent Surveillance-Broadcast
CDF	Cumulative Density Function
CFD	Clutter Flux Density
CPDR	Clutter Probability of Detection Ratio
DAA	Detect And Avoid
EO	Electro-Optical
EO/IR	Electro-Optical/Infrared
FAA	Federal Aviation Administration
FTF	False Track Flux
GBR	Ground Based Radar
GCS	Ground Control Station
IFR	Instrument Flight Rules
LoWC	Loss of Well Clear
MROF	Missed Relevant Object Flux
MRTF	Missed Relevant Track Flux
MSU	Mississippi State University
NAS	National Airspace System
NF	Navigable Fraction
NMAC	Near Mid-Air Collision
OSU	Ohio State University
rDAA	Raspet Detect And Avoid
sUAS	Small Uncrewed Aircraft System
TCAS	Traffic Alert and Collision Avoidance System
UAS	Uncrewed Aircraft Systems

## EXECUTIVE SUMMARY

This report presents a comprehensive evaluation of Detect and Avoid (DAA) systems for Uncrewed Aircraft Systems (UAS), focusing on their performance and safety in cluttered environments. By integrating modeling, simulation, and experimental data, the study addresses the operational challenges of environmental clutter, assesses key risk metrics, and proposes actionable recommendations for system improvement. The primary objective is to evaluate how DAA systems manage conflicts with intruder aircraft under varying clutter densities while maintaining operational suitability and safety.

Risk assessments are based on metrics combining the severity and likelihood of hazard outcomes, including Near Mid-Air Collision (NMAC) probability and Loss of Well Clear (LoWC). Two key datasets form the basis of the simulations. The Glendale Encounter Set provides 665,000 enroute scenarios to replicate package delivery flights interacting with real-world Automatic Dependent Surveillance-Broadcast (ADS-B) traffic, while the MIT Terminal Area Dataset focuses on terminal operations near airports. These datasets enable the simulation of diverse operational conditions critical to assessing DAA performance.

Environmental clutter, defined as non-relevant noise or false targets, significantly impacts DAA system reliability. Metrics such as Clutter Flux Density, Clutter Risk Ratio, and Navigable Fraction quantify clutter's effects, highlighting increased alert rates and sensor workload. To better understand and mitigate these effects, synthetic clutter environments were generated using real-world data, with densities ranging from five false tracks/(nm<sup>2</sup>-hr) (rare encounter) to 470 false tracks/(nm<sup>2</sup>-hr), (frequent and often multiple targets).

Simulations were conducted using CAL Analytics' environment, incorporating ACAS sXu and Rasper DAIDALUS DAA algorithms. Enroute simulations with varying clutter densities reveal that while clutter alerts are often short-lived and do not frequently lead to LoWC or NMACs, they considerably raise the total alert duration, potentially impacting remote pilots in command or Air Traffic Control (ATC). The study found that the presence of clutter occasionally forced early evasive actions, inadvertently reducing the frequency of some LoWC events but increasing overall workload and airspace complexity.

Terminal operations are especially vulnerable to clutter. Clutter significantly disrupts flight path stability and increases the likelihood of missed approaches and erratic guidance cues, even with low levels of average clutter flux density (< 13 false tracks/(nm<sup>2</sup>-hr)). Filtering mechanisms reduced false clutter alerts but did not entirely address operational challenges in high-clutter scenarios.

Pilot surveys from field tests show that environmental clutter, such as non-relevant tracks and noise, significantly increases alert rates and operational complexity. Filtering strategies reduce false alerts but fail to completely mitigate challenges in high-clutter environments. Field tests emphasize the limitations of cooperative sensors like ADS-B, which often generate nuisance alerts from ground-based traffic.

The report concludes with actionable recommendations to enhance DAA system performance. These include refining algorithms to dynamically filter clutter, optimizing sensor placement for better detection accuracy, and equipping ground control stations with customizable interfaces to reduce pilot distractions. Future work will expand testing to high-density airspace and integrate stochastic trajectory models to better represent real-world conditions.

# **1 INTRODUCTION & BACKGROUND**

## **1.1 Final Report Overview**

This report provides a comprehensive analysis of the performance and safety of Detect and Avoid (DAA) systems for Uncrewed Aircraft Systems (UAS) under varying operational conditions. It focuses on the challenges posed by environmental clutter and assesses mitigation strategies through modeling, simulations, and experimental data collection. Key components of the report include the evaluation of risk metrics, encounter datasets, clutter modeling, simulation results, and operational suitability analyses.

## **1.2 Risk Metrics and Encounter Datasets**

The analysis employs composite risk metrics, incorporating severity and likelihood of hazard outcomes, to evaluate DAA system performance. Two major datasets—the Glendale and MIT Terminal Area encounter sets—are used to simulate realistic operational conditions. These datasets feature thousands of unique trajectories for both ownship and intruder vehicles, designed to replicate diverse scenarios such as terminal operations and enroute flight.

## **1.3 Simulation Environment and Algorithms**

Simulations are performed using CAL Analytics' fast-time simulation environment, integrated with ACAS sXu, a specialized DAA algorithm for small UAS. The Raspnet DAA algorithm is also explored for its efficiency in conflict detection and avoidance, particularly in complex airspace with high traffic density. Key metrics like Near Mid-Air Collision (NMAC) probability and Loss of Well Clear (LoWC) are evaluated to verify the efficacy of these systems.

## **1.4 Clutter Modeling and Impact Analysis**

Clutter is a significant challenge in DAA systems, potentially causing false detections and increasing the risk of collisions. The report introduces metrics such as Clutter Flux, Clutter Risk Ratio, and Navigable Fraction to quantify clutter's impact. Simulated clutter environments, ranging from low to high density, are generated using statistical methods to assess system reliability. Results reveal that high clutter density reduces navigable and in encounters predesigned to generate an alert, actually lead to lower alerts due to the aircraft maneuvering ahead of the encounter. While this is a simulation artifact, it should be taken into consideration for the design of DAA algorithms to ensure the vehicle returns to its original course in a timely manner. These findings point to the necessity of considering specific DAA instantiations when considering the impact of clutter on overall safety metrics.

## **1.5 Experimental Data Collection**

Field tests utilizing the Iris Automation Casia G sensor system demonstrate real-world clutter detection and avoidance. The experiments, conducted in rural and suburban environments, highlight the importance of sensor placement and the challenges of distinguishing clutter from true intruder tracks.

## **1.6 Operational Suitability and Safety**

Safety analyses reveal the trade-offs between operational suitability and risk mitigation. While clutter increases alert rates and operational workload, examples of using filtering in conjunction with different detection algorithms are proposed to improve safety margins without overburdening the automated DAA systems or Air Traffic Control (ATC). Terminal operation simulations further underscore the need for tailored strategies to handle high-clutter environments effectively.

## 1.7 Pilot Surveys

Section 5 details pilot survey results from a limited series of tests conducted by Mississippi State University (MSU) to assess the impact of clutter on DAA system usability in the terminal environment. These tests supplied researchers with field data on true and false detections to inform future simulation modeling. After the flight test program concluded, pilots and flight test engineers were surveyed to gather qualitative feedback on the overall user experience, troubleshooting challenges, and the impact of clutter on maintaining safe separation from manned aircraft.

## 1.8 Risk Metrics

Detailed evaluation of risk is based on the composite of severity and likelihood of a hazard outcome, identifying hazards and hazard outcomes, and evaluating mitigations and residual risks. The primary outcome of interest is reduced separation between ownship and crewed aircraft, with risk assessments aligned to recent guidance and severity/likelihood tables.

The DAA implementation will first be verified using the metrics (shown in Table 1) by comparing the results with those obtained in the ACAS sXu operational validation report published by Traffic Alert and Collision Avoidance System (TCAS) Program Office. The metrics presented in Table 1 will be expanded in Section 3, which are used to assess the impacts of clutter on system performance and safety.

Table 1. Analysis Metrics.

Primitive Metrics	Safety Metrics	Operational Suitability Metrics
Horizontal Range	P(NMAC) Probability of NMAC	Alert Rate
Vertical Range	P(LoWC) Probability of LoWC	Reversals
Slant Range	NMAC Risk Ratio	Splits
Closest-Point-of-Approach	LoWC Risk Ratio	Alert Durations
Time of Closest-Point-of-Approach		
Horizontal Miss Distance		
Vertical Miss Distance		
Near Mid Air Collision (NMAC)		
Loss of Well Clear (LoWC)		
Severity of LoWC (SLoWC)		

## 1.9 Encounter Sets

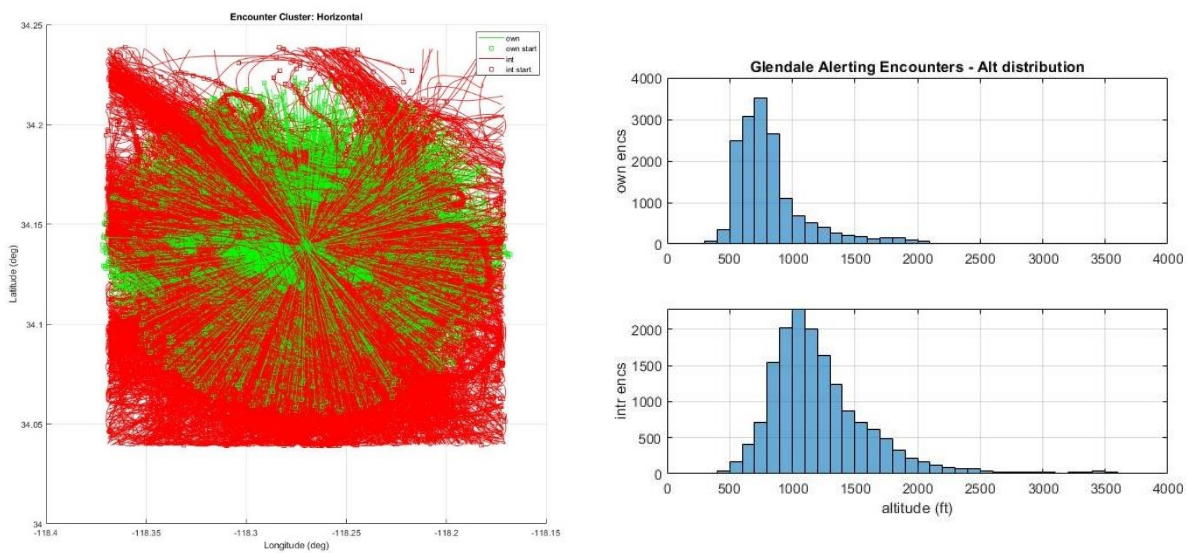
For fast-time simulations, a broad encounter set was chosen to allow for the incorporation of different clutter densities as outlined in the previous sections. Down selection of existing datasets showed that the TCAS/MITRE dataset used in characterizing sXu was a suitable candidate as the range of vehicle speeds and altitudes were commensurate with the operating environments considered in this work. The following sections detail the datasets and sampling used in the remainder of this report.

### 1.9.1 Glendale Encounter Set

The encounters used for this task are drawn from the Glendale Hub-and-Spoke encounters [OPVAL]. These encounters feature an ownship vehicle simulating a package delivery, together with an intruder vehicle trajectory obtained from actual Automatic Dependent Surveillance-

Broadcast (ADS-B) traffic observed in the National Airspace System (NAS) and provided by the TCAS Program Office and MITRE. 20,000 unique ownship vehicle trajectories radiate at 20-40 kts from a warehouse in Glendale, CA, at uniform headings from 0 to 359 degrees over a range of approximately 3 nm, and a set of 26,845 ADS-B intruder trajectories are paired with them to form a total of 1,000,000 encounters that include take-off, enroute flight, and landing. Horizontal and vertical miss distances are used to guide the pairing of ownship and intruder trajectories, with the pairing being rejected if not within 5 nm and 3,000 feet, respectively. This full set is provided together with a reduced set of roughly 665,000 encounters that only include the enroute portion and removal of some duplication. The reduced set was used for this effort.

The encounters were further reduced by selecting 1) a non-alerting encounter set that did not result in vehicle-on-vehicle alerting (used to quantify an increase in alert rate due exclusively to clutter), and 2) an alerting encounter set that did result in vehicle-on-vehicle alerting (used to investigate both operational suitability and safety metrics). Initial simulations of all 665,120 encounters were performed resulting in approximately 12,000 alerting encounters. About 2,000 of these alerted within the first five seconds and were discarded. An additional 10,000 non-alerting encounters were chosen at random. Figure 1 is a composite plot showing the geographic location of the one-on-one encounters, with the ownship trajectories in green and intruders in red.



(a) Ownship & Intruder Top-down View

(b) Ownship & Intruder Vertical Profile

Figure 1. Glendale alerting encounter set.

### 1.9.2 MIT Terminal Area Encounter Set

Terminal encounters were simulated using the MIT Lincoln Labs terminal environment datasets. These encounters were developed using a Bayesian network-based model specifically tailored for assessing the safety performance of DAA systems for UAS. The ownship trajectories focus on straight-in approaches at single-runway Class D airports. Using Federal Aviation Administration (FAA) radar data from 2015, the model incorporates structured correlations between aircraft trajectories and generates one million simulated encounters for safety analysis. Current assumptions include the ownship is an uncrewed aircraft operating under Instrument Flight Rules

(IFR) on straight-in approach, interactions are limited to a single intruder aircraft either landing or taking off, and trajectories are limited to 8 NM and 3000 ft above the airfield. The dataset includes trajectory data in binary and text formats, along with encounter conditions and closest point of approach information.

### 1.9.3 Cooperative Surveillance Parameters

The surveillance parameters used for the ownship and intruder aircraft are shown in Table 2. The ownship vehicle surveillance is modeled as being GPS quality, while the intruder model uses a lower-accuracy ADS-B model. Uncertainty models for track sensors are given in Table 3. Of note, different sensor modalities (such as ground-based acoustic, onboard radar, etc.) have drastically different error statistics which will impact the results presented in Section 5. However, the sensors presented below represent two common DAA solutions outside of cooperative sensing schemes with error bounds commensurate with ground-based radar and airborne Electro-Optical/Infrared (EO/IR) standards.

Table 2. Ownship and Intruder Vehicle Surveillance Parameters.

Vehicle	Interface	Lateral Accuracy (ft)	Velocity Accuracy (knots)	$\sigma_{alt}$ (ft)	Note
Ownship	WGS84	10	3	1.5	Gaussian Noise
Intruder	ADS-B 978 UAT	8	1	4.7	Gaussian Noise

Table 3. Surveillance Sensor Uncertainty.

Vehicle	Interface	Lateral Accuracy (ft)	Velocity Accuracy (knots)	$\sigma_{alt}$ (ft)	Note
Ground based radar	ASTERIX	200	10	50	Range dependent error statistics. Averages presented in table.
EO/IR	-	50	12	100	Detailed modeling statistics listed in Figure 32.

## 1.10 Fast-Time Simulation Environment

### 1.10.1 Enroute Encounters

Simulations were performed using CAL Analytics' in-house fast-simulation environment built around the AFSIM developed by the Air Force Research Lab. CAL has integrated a range of DAA algorithms, sensor models, and custom add-ons with AFSIM. For the clutter simulations considered in this work, sXu was the chosen variant of the ACAS, a version of the system specifically developed for small Uncrewed Aircraft Systems (sUAS). This DAA system has been integrated with CAL's fast simulation environment. The well-clear definition for sUAS vs crewed aircraft is 2000-ft horizontal and 250-ft vertical with no tau component. The NMAC definition is 500-ft horizontal and 100-ft vertical. Verification of the efficacy of ACAS sXu guidance is given by showing that separation between the ownship and intruder vehicle increases for when using the ACAS sXu mitigation, as shown in Figure 2.

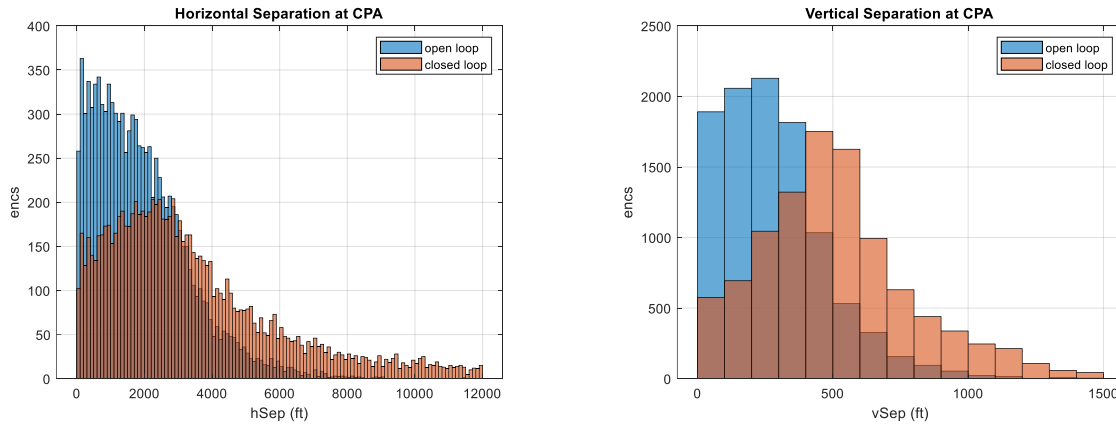


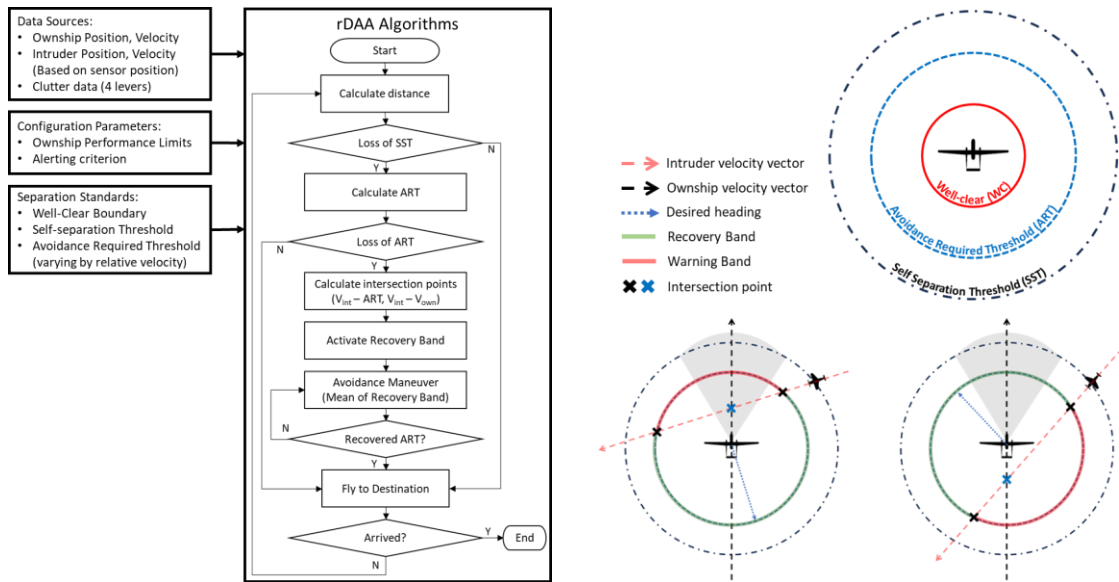
Figure 2. Horizontal and Vertical Separation: ACAS sXu Mitigation (closed-loop) vs Unmitigated (open-loop).

### 1.10.2 Terminal Operations

In this report, the Raspnet Detect and Avoid (rDAA) algorithm, developed in-house based on the core concepts of DAIDALUS, was applied. DAIDALUS provides a robust framework for conflict detection and resolution in UAS, but its extensive calculations for each potential conflict can become computationally expensive, particularly in complex airspace environments with multiple intruders. To optimize this process, the rDAA algorithm simplifies the calculation by focusing on two key elements: the avoidance required threshold and the two crossing points of the intruder's trajectory. By narrowing down the decision-making process to these two parameters, the algorithm reduces the need for intensive, continuous calculations while still maintaining a high degree of accuracy in detecting and avoiding potential conflicts.

The rDAA system offers several key features that enhance its efficiency and effectiveness in conflict avoidance. It determines an "Avoidance Required Threshold" based on the relative speed, distance, and predicted positions of the ownship and intruder, ensuring that evasive maneuvers are only initiated when necessary to minimize unnecessary actions and optimize safety margins. Instead of continuously analyzing the entire flight trajectories, the algorithm focuses on two critical crossing points where the intruder's path intersects with the ownship's predicted course, allowing for precise conflict risk assessment and timely avoidance guidance. This approach significantly reduces computational load, making the Raspnet DAA suitable for real-time applications in both low- and high-traffic environments. Its streamlined design ensures efficient decision-making, even in complex airspace scenarios with multiple potential conflicts, without sacrificing accuracy or timeliness.

Figure 3 shows the flowchart of the rDAA, illustrating the alert ranges and operational concepts. This system compares the position, speed, and heading angle of intruders and clutter within the self-separation threshold (10,000 ft) to those of the ownship to prepare for collision avoidance. When an intruder enters the fixed Avoidance Required Threshold (6,500 ft) range, the system identifies the intersection between the ART boundary and the intruder's heading vector, generating a recovery band. It then suggests the midpoint of this band as the desired heading to guide avoidance maneuvers.



(a) rDAA algorithm flowchart

(b) Parameters and operation concept

Figure 3. Raspet Detect and Avoid System.

## 1.11 Clutter Metrics

The evaluation of clutter and its impact on UAS navigation and detection performance is crucial—particularly for DAA systems. This section outlines several key metrics developed for clutter analysis and their importance in system performance evaluations.

### 1.11.1 Types of Clutter in the Air Picture and Their Operational Impact

In radar-based air picture systems, clutter can be categorized based on its duration, movement, and persistence within the monitored space. Understanding these distinctions is critical as different types of clutter have varying implications for safety and operational performance, particularly in aviation or airspace management systems

#### 1.11.1.1 Persistent Long-Duration Clutter

Persistent clutter refers to objects or signals that remain in the radar air picture for an extended period of time. This type of clutter often results from stationary or slowly moving objects such as terrain, tall structures, wind turbines, or atmospheric phenomena (e.g., temperature inversions or moisture layers) that consistently reflect radar signals.

#### 1.11.1.2 Flux Clutter (Dynamic Entry and Exit)

Flux clutter refers to clutter that enters and exits the radar air picture intermittently. These objects may appear for short or moderate durations and then disappear. Examples include moving vehicles, birds, drones, or transient weather events like moving rain showers or small storms.

#### 1.11.1.3 Short-Duration Clutter (Sparkle)

Short-duration clutter, often referred to as "sparkle," describes clutter that appears very briefly and then promptly disappears. Sparkle clutter can be caused by environmental factors such as electromagnetic interference, fast-moving objects (e.g., birds or small drones briefly entering the radar beam), or temporary reflections from atmospheric disturbances.

#### **1.11.1.4 Comparative Effects of Different Clutter Types**

Each type of clutter—persistent, flux, and sparkle—can have different effects based on where it occurs in the air picture and how it behaves over time:

##### *1.11.1.4.1 Critical vs. Non-Critical Zones:*

Clutter in the approach path or near navigation zones poses a greater safety risk than clutter located in non-critical portions of the airspace, where operational concerns are less stringent.

##### *1.11.1.4.2 Duration and Density:*

A single persistent clutter track may be easier to classify and mitigate compared to a large number of small, short-duration clutter tracks moving dynamically. High clutter density (even transient) can overwhelm radar systems, whereas long-duration clutter may have more localized but persistent impacts.

#### **1.11.2 Clutter Flux**

Clutter Flux quantifies the dynamic behavior of clutter in a given area or volume over time. It measures how frequently clutter appears in a specific region and is calculated as

$$cf = nc / \Delta t$$

Where  $nc$  is the total number of clutter elements detected in a defined region (area or volume) during the time interval  $\Delta t$ . Clutter flux is crucial for understanding the rate of clutter appearance in the operating environment and assessing how dynamic the clutter behavior is over time. This information helps evaluate the overall flow of clutter and its potential impact on UAS operations, particularly in environments with frequent false or non-relevant objects.

Clutter Flux quantifies the overall flow of clutter into a defined region over a given time period. It measures how frequently clutter elements appear, providing insights into the dynamic behavior of clutter within the operating environment. A higher clutter flux means more false objects are detected in the environment, which can overload a system's detection and tracking capabilities. Clutter flux is a direct measure of how dynamic the clutter is in the operating environment. It helps with understanding how clutter changes over time and how it impacts sensor workload. In high-clutter environments, the system could be flooded with false objects, increasing the likelihood of near misses or collisions, as relevant targets might be obscured by clutter or avoidance against real targets is degraded. A lower clutter flux generally results in safer operating conditions as the system can more easily detect and avoid real objects. By monitoring clutter flux, systems can adjust their detection thresholds or filtering mechanisms dynamically, improving operational efficiency by reducing false positives. Including clutter flux as a benchmark for comparing a system's performance in different environments or with different sensors as well as analyzing how clutter flux correlates with system alert rates and false detection events seems like a good approach.

#### **1.11.3 Clutter Flux Density**

Clutter Flux Density (CFD) measures the intensity of clutter flow in a defined area (or volume) over time. It provides a normalized rate, indicating how densely clutter elements appear within a given space. It helps quantify the amount of clutter a system must process, which directly affects detection, tracking, and navigation performance.

$$cfd = \frac{nc}{A * t}$$

Where  $nc$  is the number of clutter elements in the area or volume,  $A$  is the area (or volume) in which the clutter elements are present, and  $t$  is the time interval over which clutter is measured.

High clutter flux density indicates a cluttered environment where a large number of false objects appear within a small area or volume in a short time. This leads to an increased workload for sensors and detection algorithms, potentially reducing system performance or increasing the chances of false alarms. Low clutter flux density suggests that fewer clutter elements are present, making it easier for systems to detect relevant objects and reducing false detections. CFD provides a measurable way to evaluate how much clutter a system must deal with, enabling comparison of different environments or sensor performance. For DAA systems, a high CFD may result in more false detections or missed targets, increasing the risk of mid-air collisions or near misses. Knowing the clutter flux density helps with designing better sensor filtering mechanisms and improving decision-making algorithms for handling clutter-laden environments.

Later in the report, an experiment where ground-based radar and EO/IR systems were used to calculate clutter flux is discussed. A value such as 260 false targets  $\text{nm}^{-2} \text{hr}^{-1}$  are reported, as are the effects of clutter on safety metrics like LoWC and NMAC. This experiment directly applies to CFD and can provide insights into how clutter density impacts system performance.

#### ***1.11.4 Clutter Clustering***

Clustering refers to how clutter objects are spatially and temporally grouped together, significantly impacting operational safety and suitability. While average clutter metrics provide a broad understanding of clutter distribution across an entire region, localized clustering highlights areas where clutter density is exceptionally high in critical zones. These localized clusters can occur in approach paths, navigation corridors, or other operationally significant regions, creating challenges that may not be apparent when analyzing regional averages alone.

The proximity and density of clutter objects in such localized clusters directly reduce the available maneuvering space for UAS. In these high-density areas, sensors may become overwhelmed, making it difficult to distinguish real targets from clutter and increasing the risk of near misses or failure to maintain well-clear conditions.

For example, an environment with low average clutter across a region may still have "hot spots" of high clutter density where UAS operations become unsafe. Assessing localized clustering is crucial for identifying these critical areas, as they require targeted solutions such as:

- Strategic sensor deployment to improve coverage in high-clutter zones.
- Adaptive detection algorithms that focus on critical clusters while ignoring low-density regions.
- Resource allocation adjustments, such as prioritizing computational power or sensor sensitivity in clustered areas.

Understanding both average clutter metrics and localized clustering patterns provides a more comprehensive assessment of the operating environment. By addressing localized clustering, systems can mitigate the operational risks posed by dense clutter regions and ensure safer, more reliable UAS performance.

### ***1.11.5 Navigable Fraction***

The Navigable Fraction (NF) represents the portion of the airspace or volume that remains free of clutter, allowing safe maneuvering. It is given by the ratio of the navigable area or volume to the total area or volume

$$NF = A_N / A_T$$

or

$$NF = V_N / V_T,$$

where  $A_N$  and  $V_N$  are the navigable area and volume, respectively, and  $A_T$  and  $V_T$  are the total area and volume, respectively. This metric is expected to vary with time as the amount of clutter varies and as the separation between clutter elements varies. A high  $NF$  means more of the environment is available for safe maneuvering, while a low  $NF$  indicates clutter is restricting movement. This metric helps assess the usable space for UAS to operate without encountering clutter, aiding in route planning and maneuverability analysis. A low  $NF$  increases the risk of collisions or near misses as UAS have less space to navigate. Maintaining a high  $NF$  ensures that UAS can safely avoid both clutter and other aircraft. Systems can use  $NF$  to plan optimal flight paths and avoid cluttered areas, leading to more efficient operations. In real-time systems, monitoring  $NF$  helps adjust navigation strategies dynamically.

In this report's conclusion, an approach where clutter clustering based on sensor data from the environment is mentioned, which is used to simulate the reduction in  $NF$  as clutter density increases. This shows how clustering affects available space for safe maneuvering.

### ***1.11.6 Clutter Risk Ratio Delta***

This metric assesses the change in risk between cluttered and non-cluttered environments. It is calculated as

$$\Delta RR = RR_{CLUTTER} - RR_{NO CLUTTER}.$$

By comparing the risk ratios, operators can determine how much more likely a near-miss or collision becomes in the presence of clutter, which is vital for safety assessments. A high delta means clutter significantly increases the risk of incidents, while a low delta suggests clutter has little impact. It is a direct indicator of how much clutter increases the operational risk, making it useful for risk assessments and safety planning. This metric helps determine if and when systems need to deploy more advanced filtering or detection mechanisms so that the ability to avoid other aircraft is not degraded.

### ***1.11.7 Clutter Probability of Detection***

Clutter Probability of Detection Ratio (CPDR) compares the likelihood of detecting an object in a cluttered environment versus a non-cluttered one and is given by

$$CPDR = PD_{CLUTTER} / PD_{NO CLUTTER}.$$

Here, PD refers to the Probability of Detection, which measures the likelihood of correctly detecting an object (e.g., an aircraft) in the presence of clutter. A CPDR closer to one indicates

that clutter has minimal impact on detection, while a low CPDR suggests that clutter significantly hinders detection performance, increasing the risk of missed detections and safety violations.

However, it is important to extend this analysis to the Probability of Track (PT). While detection refers to identifying objects in the sensor's field of view, tracking involves maintaining continuity across detections over time to form a reliable trajectory. Tracking systems are often limited by computational resources or algorithmic constraints and may struggle to differentiate between clutter and true targets. Issues such as:

Track stealing (where a track intended for an aircraft gets associated with clutter),

Track splits (where a single track mistakenly breaks into multiple tracks), or

Track merges (where clutter and target detections are combined),

can cause disruptions in maintaining reliable tracks. These errors often occur in cluttered environments where overlapping detections challenge the tracker's ability to resolve objects accurately.

Furthermore, there is a distinction between the Probability of Track and the Probability of a Classified Track of Sufficient Maturity. Even if a track is initiated, it may not reach the maturity required to be passed on to higher-level alerting and avoidance algorithms. Maturity involves ensuring the track is consistently reliable, well-classified (e.g., as an aircraft vs clutter), and stable enough to influence operational decisions.

In summary, while CPDR evaluates the raw detection performance in clutter, the Probability of Track and Probability of Classified Track highlight the added challenges in:

Forming and maintaining stable tracks, resolving clutter from true targets, and Ensuring tracks are mature enough to contribute to collision avoidance systems.

Systems with low CPDR or low track probabilities in cluttered environments may need to:

Optimize detection and tracking algorithms, Implement filtering techniques to reduce clutter-induced track errors, and Improve resource allocation to prioritize true targets over clutter.

By addressing both detection and tracking aspects, a more comprehensive evaluation of system performance in cluttered conditions can be achieved, ensuring operational safety and reducing the risk of false alarms or missed targets.

### ***1.11.8 Missed Object and False Track Flux***

Metrics such as Missed Relevant Object Flux (MROF) and False Track Flux (FTF) provide insight into the effectiveness of detection systems. MROF evaluates how many relevant objects are missed due to clutter, while FTF quantifies how many false tracks are generated. Both metrics are calculated using the normalized number of missed objects or false tracks in a given area over time as

$$MROF = n_M / \Delta t$$

and

$$FTF = n_F / \Delta t,$$

where  $n_F$  and  $n_M$  represent the normalized number of false tracks and missed objects, respectively.

These metrics quantify the rate at which relevant objects are missed or false tracks are generated in a cluttered environment. High values indicate poor system performance. These metrics are crucial for evaluating detection and tracking reliability. A system with high MROF may require recalibration, while high FTF indicates issues with clutter filtering. Missing relevant objects can lead to serious safety incidents, while generating false tracks increases system workload and may cause unnecessary maneuvering, leading to inefficiency and potential hazards. These metrics help identify inefficiencies in a system's clutter management, allowing for better resource allocation and more reliable detection performance. The ground-based radar and EO/IR systems discussed herein provided data on missed objects and false tracks, which were analyzed under varying levels of clutter to determine system performance.

#### ***1.11.9 Missed Relevant Track Flux***

Missed Relevant Track Flux (MRTF) measures the number of relevant tracks missed in the cluttered environment over time (and is formulated similarly to MROF). This metric is key for tracking system performance, particularly in dense clutter scenarios where relevant objects may be difficult to differentiate from clutter. A high MRTF suggests that clutter is obstructing a system's ability to track real objects. This metric provides insight into the tracking performance of a system, especially in complex or dense environments where clutter may prevent the system from following important objects. Track classification plays a crucial role here, as the ability to differentiate between clutter tracks (non-aircraft) and relevant tracks (real aircraft) directly impacts MRTF. In environments where the number of non-aircraft tracks is significantly higher than real aircraft tracks, the importance of accurate classification cannot be overstated. Track classification is essential not only for safety analysis but also for managing the track capacity of the system. Many DAA systems define requirements based on the expected number of aircraft in the operating environment, often underestimating the additional load caused by clutter tracks. Missing relevant tracks can increase accident risk, particularly in environments where constant tracking is required for safe navigation. A high MRTF highlights a critical issue in maintaining safe operations. By monitoring MRTF, tracking algorithms can be adjusted to ensure that real objects are not missed, leading to more efficient and reliable operations.

#### ***1.11.10 Probability of Retained Clutter***

The probability that clutter is retained by the system,  $P_{clutt\_kept}$ , is important for understanding how often clutter is falsely classified as a relevant object. This metric is closely related to another metric, Probability of Non-Clutter Return Removal, which assesses how often relevant objects are mistakenly removed by the system. Ideally, both probabilities should be minimized to ensure accurate clutter filtering and reliable object detection. This metric represents the likelihood that a system fails to remove clutter from its detection or tracking processes. A high probability of retained clutter indicates poor clutter filtering. It helps with the evaluation of a system's ability to filter out irrelevant or false objects, which is essential for reducing false alarms and focusing on relevant targets. If clutter is retained, false alarms and unnecessary maneuvers can result, increasing the risk of confusion and collisions. Ensuring low retention of clutter is important for maintaining safety. Reducing retained clutter improves system efficiency by ensuring resources are focused on real objects, not false positives.

### 1.11.11 Summary

These clutter characteristics and system performance metrics provide a comprehensive framework for evaluating the impact of clutter on UAS DAA systems. By assessing factors like clutter flux, clutter flux density, clustering, and detection probabilities, these metrics enable a thorough analysis of system capabilities and risk, leading to safer and more reliable autonomous aircraft operations.

## 2 SENSOR DATA COLLECTION AND ANALYSIS

### 2.1 Introduction

The following sections detail the collection of field data, modeling, and simulation of clutter in realistic environments. Data collection spanned several months and was enhanced by various ongoing DAA-related programs at MSU and the Ohio State University (OSU). MSU collected ground-based and airborne Electro-Optical (EO) DAA sensor data, ground-based small form factor radar, and ground-based acoustic array data while OSU's efforts focused on the collection of wide-area ground-based radar data. The following section discusses the collection of ground-based EO and radar data but only includes the efforts and results of modeling ground-based EO data. Future work will include modeling the remaining other DAA sensors.

### 2.2 Iris Automation's Casia-G Sensor

Iris Automation's Casia G was used for the second half of MSU's A57 clutter data collection. This system is a 14in L x 11.5in W x 6in H stationary ground-based aircraft detect and alert system with varying mount functionality (wall, pole, etc.) It makes use of a built-in ADS-B system and six cameras to obtain real-time data on multiple tracks (airplanes, helicopters, drones, etc.) It provides full optical, 360° field of view for detections, remote Pilot in Command access, a possibility for a mesh network for larger coverage, and unlimited range and maximum single node range of 3024m (about 1.88 mi).



Figure 4. IRIS Automation's Casia G. Sensor (left), Judy power supply system (center) and SIERRA wireless router (right).

#### 2.2.1 Methodology and Safety Measures

Safety risks were minimal for Casia G data collection. Almost all risks were environmental (heat, insects/bugs, tripping hazards). Most of the data collection that occurred during A57 took place during a pre-planned flight test by Raspet. The researchers' interest lies in observing "non-cooperative" intruders, so any part of the log files where the ownship was present, was removed. To achieve this, the times when the ownship entered and exited the test area were recorded. These matching timestamps were then located in the log files, and that time block was removed. Again,

this procedure was only done for data collected during a known flight test. This data was collected at two different MSU-owned “farms”, North Farm and South Farm, located on the outskirts of Starkville. These sites were chosen because they gave researchers a chance to collect in a “rural” environment. Some of the collected data occurred on top of Rice Hall on the campus of MSU. This site was chosen due to Rice being one of the taller buildings on campus, with mostly unobstructed views, and also accessible due to ongoing construction. Researchers wanted to test if the Casia collected any differently if stationed at a higher elevation. It also provided researchers with a more suburban environment as opposed to the farms where a large majority of the collections were taken.



Figure 5. South farm data collection location.



Figure 6. Rice Hall data collection location.

A small sample of data was collected behind the Raspet Flight Research Lab Facility, on the grounds of the KSTF airport. This data was more experimental in nature and not used for any of the analyses.

### **2.2.2 Conclusions**

All of the data collected with the Casia G systems occurred either in Starkville or just on the outskirts of the town. Due to this, the types of clutter or intruders available were mostly the same for each testing day. This being said, Starkville does have a fairly active airspace. Multirotors commonly used for research, general aviation aircraft, military aircraft, and large passenger aircraft can all be seen frequently.

While the Casia G appears to have some inconsistencies, especially when objects appear to be at the limits of its detection range, it does provide the researcher with extensive data sets, including images and recordings. The Casia G system offers a masking function for objects in the field of view that trigger false detections, but this was not used during any collections. Iris also offers an application that can provide real time intruder tracks and Casia G status.

To test if elevation difference played a role in increasing the amount or type of detections, two Casia G units were placed on top of a building on MSU's campus. It was found that this height difference did not play a significant factor in increasing or decreasing detections. Moreover, it seems that the sole difference maker in varying data sets was the amount of traffic or clutter in the airspace on that particular day. Any future data collection should ideally occur in a more populated area with a busier airspace. This would allow researchers to observe how the system handles a larger volume and wider classification range of intruders, while also refining modeling and simulation efforts.

### 2.3 EO/IR Modeling and Analysis Efforts

This manuscript summarizes MSU Industrial and Systems Engineering Department’s approach to modeling EO/IR clutter using statistics and stochastics. Even though the researchers have selected three different environmental configurations (low, medium, and high) based on the density, the underlying approach can be consistent. The goal is to simulate the EO/IR clutter using the real data using distribution fitting. Figure 7 summarizes the proposed approach.

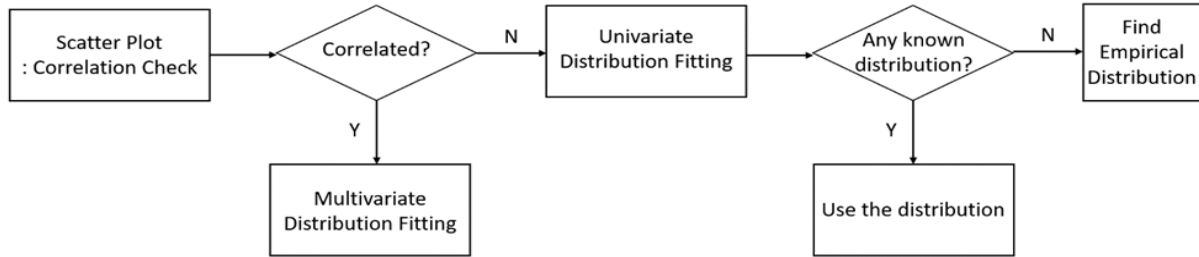


Figure 7. Clutter modeling using distributed fitting.

#### 2.3.1 Approaches Used

The first step is to check the scatter plots of all the variables (in this case, they are latitude, longitude, and altitude). If no strong correlation is observed among them, one can use univariate distribution per each variable and aggregate them later. However, if any significant correlations are observed among latitude, longitude, and altitude, then multivariate distribution should be considered. For the univariate distribution fitting, the researchers considered 22 well-known distributions (Normal, Weibull, Beta, etc.). If any of those distributions matched this clutter data set, the closest distribution was selected to generate simulated clutter. If none of them matched the real data, the team constructed the empirical distribution (cumulative density function) to simulate the clutter data set.

#### 2.3.2 Case 1: High – Max

The first case considers a high clutter-density environment, and it is required to check any correlation between all the density variables (Latitude, Longitude, and Altitude) before simulating clutter. Table 4 summarizes the correlation values between all three, and the researchers observed that there is no significant correlation. There is very little correlation observed between latitude and longitude, while altitude shows a slightly negative correlation with both latitude and longitude. This is likely because airborne data is more frequently observed at higher altitudes, which differ from ground clutter trajectories. While the team assumed the independence of the variables in this model, generalizing it to highly correlated environments would require accounting for the joint distributions of all three variables.

Table 4. Correlation between latitude, longitude, and altitude in a high clutter density environment.

Correlation (r)	Latitude	Longitude	Altitude
Latitude	1	0.02396	-0.1166
Longitude	0.02396	1	-0.1148
Altitude	-0.1166	-0.1148	1

The researchers used the Person correlation coefficient, as defined in Equation (1):

$$r = \frac{\sum_{i=1}^n (x_i - \bar{x})(y_i - \bar{y})}{\sqrt{\sum_{i=1}^n (x_i - \bar{x})^2 \sum_{i=1}^n (y_i - \bar{y})^2}} \quad (1)$$

where  $i$  represents the data index, and  $n$  means the total number of observations. Variables  $x$  and  $y$  are of interest (in our application, they will be latitude, longitude, and altitude), a bar notation means the sample average. As the  $r$  value is closer to either 1 or -1, it means two variables are significantly correlated. However, the researchers failed to observe any significant correlation among any variables.

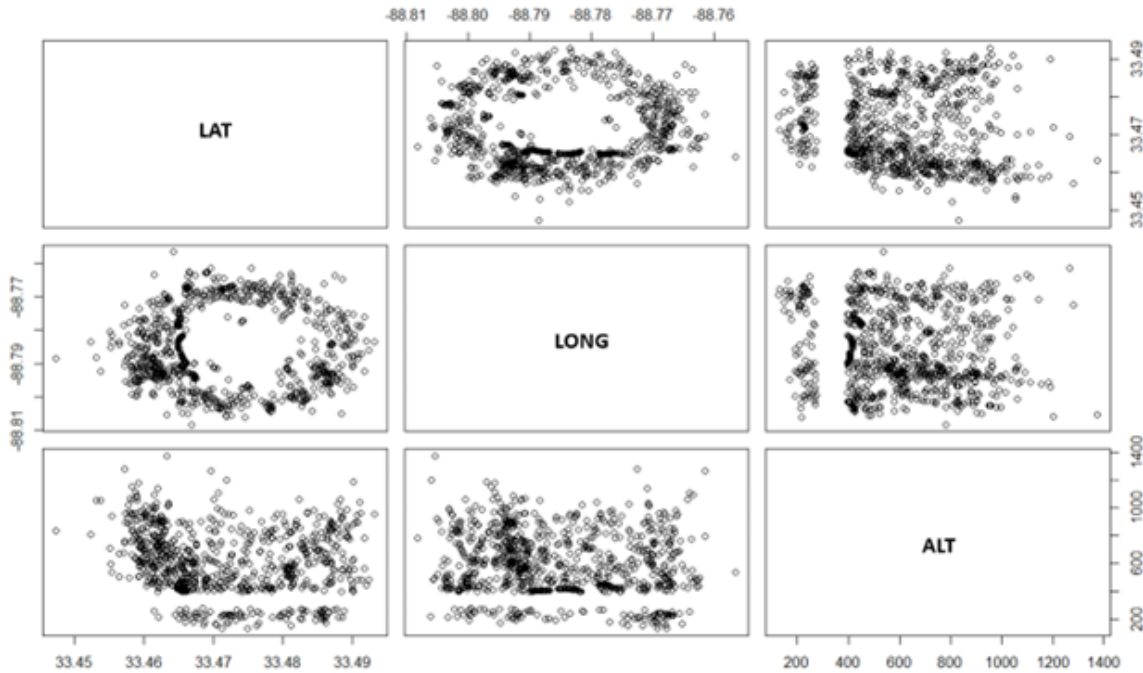


Figure 8. Scatter Plots among latitude, longitude, and altitude in a high density.

Figure 8 also provides the correlation using the scatter plot, demonstrating that no significant correlations are observed among the three variables. Thus, both Table 4 and Figure 8 support this approach to handle each variable separately. The team selected 22 well-known distributions, and they were fitted; however, none of the distributions were significant enough to demonstrate any of those three variables – Latitude, Longitude, and Altitude. Therefore, the team decided to find empirical Cumulative Density Functions (CDFs) of all three variables to simulate them.

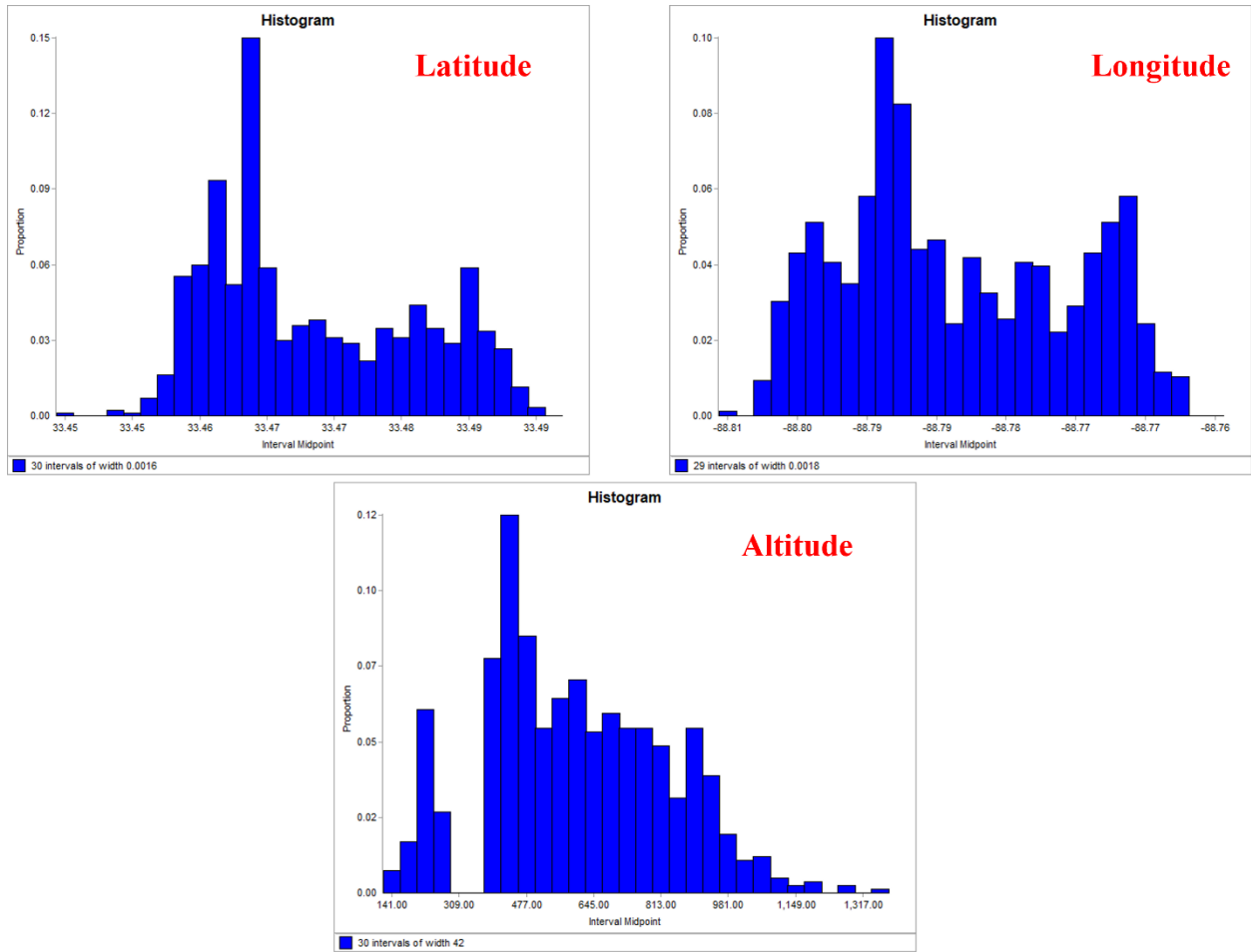


Figure 9. Histograms of (a) Latitude, (b) Longitude, and (c) Altitude in a high density.

Figure 9 depicts three histograms of Latitude, Longitude, and Altitude. From those histograms, one can observe two things: 1) each probability density function shows a combination of (more than) two distinct distributions, and 2) truncated areas in the Altitude probability density function fail to any distributions' fitting. This leads to the decision to use empirical CDFs. Algorithm 1 demonstrates the procedure to generate random numbers following a specific CDF:  $F$ .

**Algorithm 1: Random Number Generation Using Empirical CDF**

**Step 1.** Find three Empirical CDFs  $F_{Lat}(x)$ ,  $F_{Long}(x)$ ,  $F_{Alt}(x)$

**Step 2.** Generate three uniform random variables  $U_1, U_2, U_3 \sim Uniform(0,1)$

**Step 3.** Using inverse mapping  $F^{-1}$  to simulate all the variables

**Step 4.** Construct Simulated Clutter ( $Lat$ ,  $Long$ ,  $Alt$ )

Three graphs in Figure 10 illustrate three empirical CDFs of Latitude, Longitude, and Altitude. It is noted that in the CDF of Altitude, there exists a straight line from 300 to 400 miles. It represents that there were no signals detected in this altitude range. This signal “black hole” is also observed when checking the 2D representation of latitude and longitude.

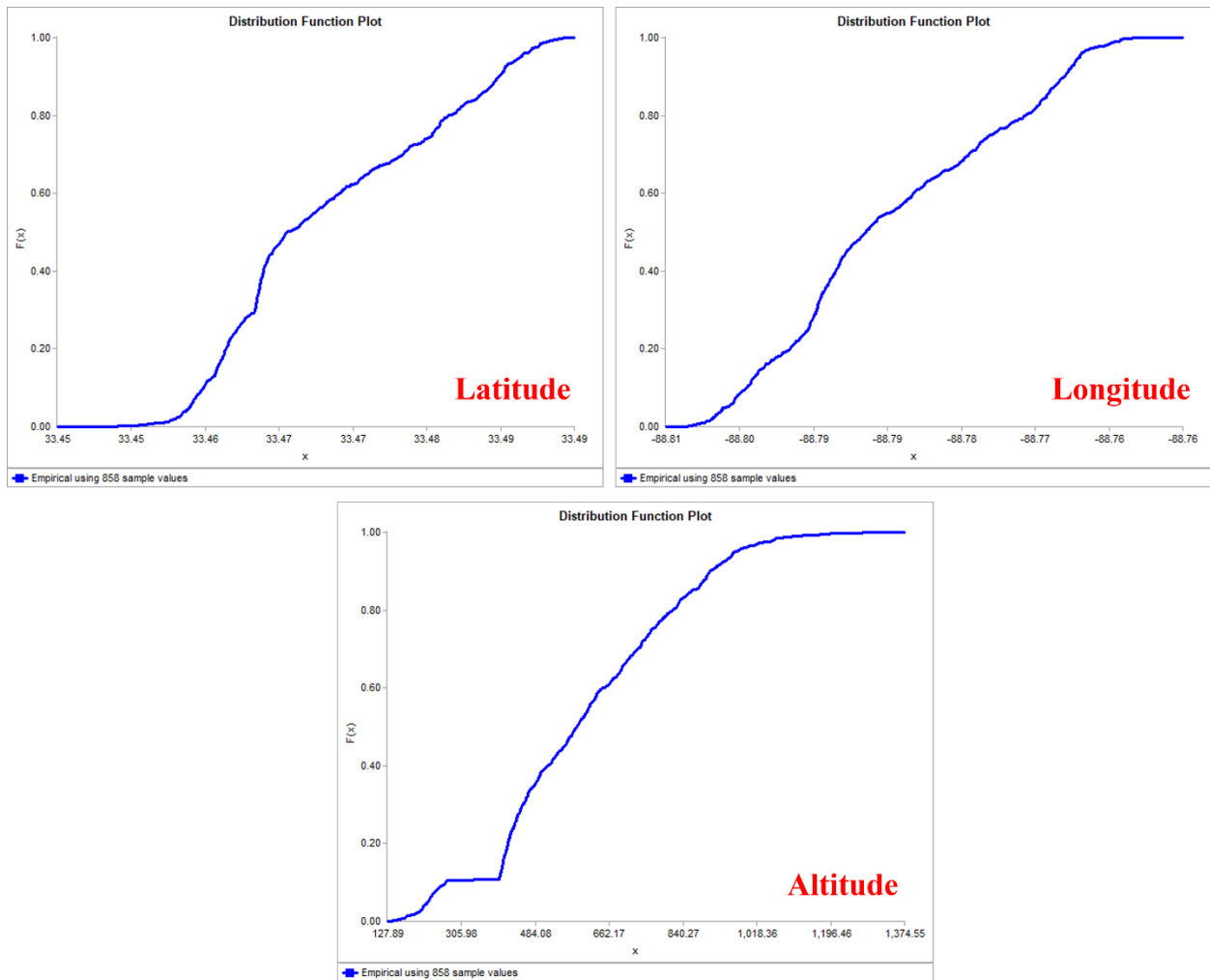


Figure 10. Empirical CDFs – latitude, longitude, and altitude in a high density.

Figure 11 compares real clutter vs simulated clutter based on empirical distribution fitting methods. The underlying pattern is roughly captured, but in the real EO/IR clutter, a “black hole” is observed in the middle of the area. If one decides to incorporate it in the simulated clutter, one can use a truncated random number generation approach by eliminating any simulated clutter located in the ellipsoid.

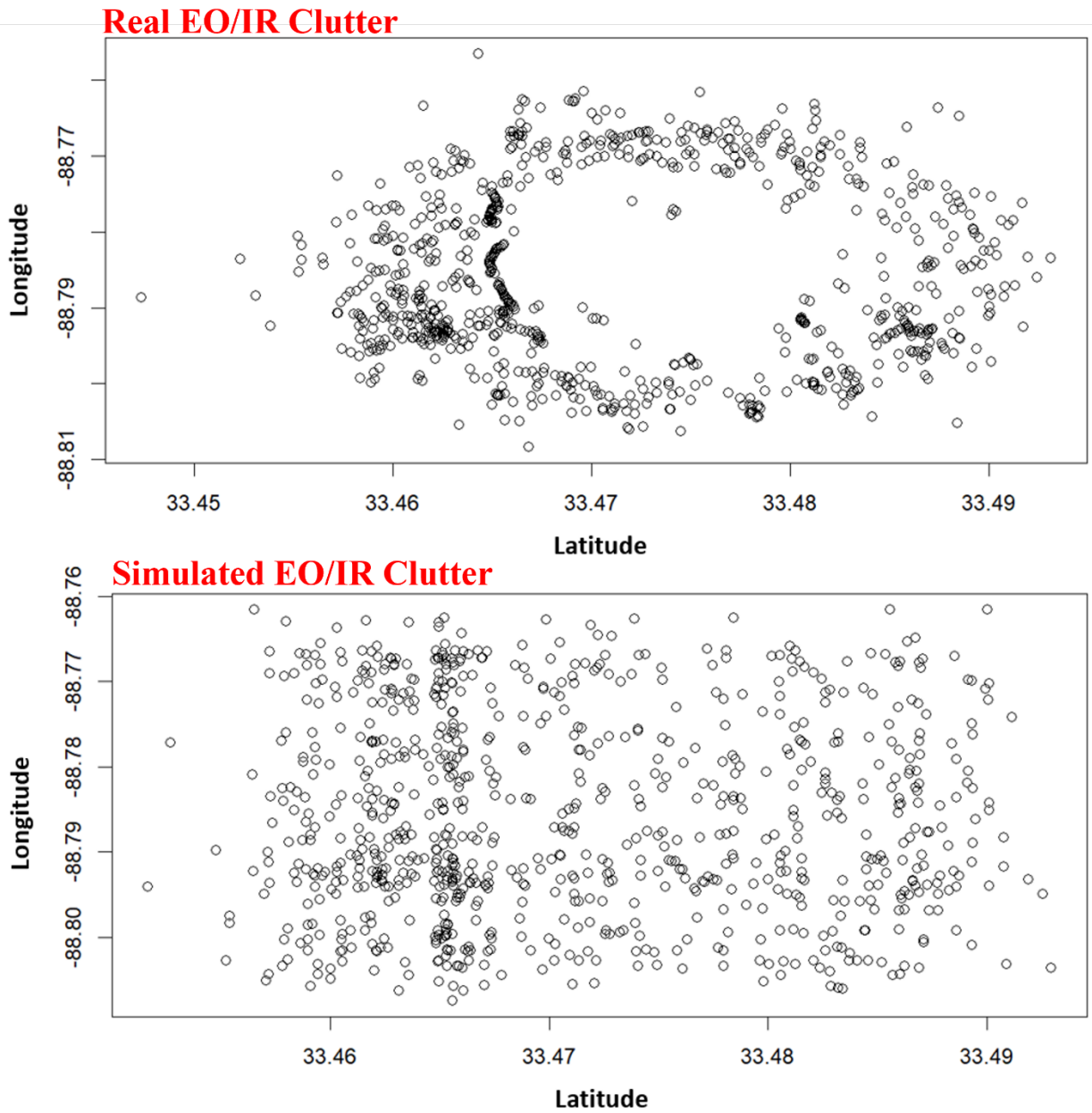


Figure 11. Real EO/IR clutter vs Simulated EO/IR clutter in a high-density.

Since the researchers removed certain altitude ranges to exclude any points due to the aircraft (not the noise), the truncated simulated clutter generation algorithm was used. Algorithm 2 summarizes the details. If one decides to exclude any clutters in a certain range of altitudes, Algorithm 2 can be used accordingly.

**Algorithm 2. Truncated Simulated Clutter Generation.**

**Step 0.** Enough number of clutters generated. Yes -> Terminate. No -> go to Step 1.

**Step 1.** Simulate Clutter using Algorithm 1.

**Step 2.** Is the clutter located in the ellipsoid?

Yes -> Remove it and move to Step 1. No -> Keep it and move to Step 1.

The medium and low levels of clutter (case 2 and case 3) are also considered, and the same techniques are applied.

### 2.3.3 Case 2: Medium

Like the first case, it is required to check whether any significant correlations are observed. As Table 5 shows, there are no significant correlations between latitude and longitude. However, altitude and latitude show a certain level of correlation. Thus, when one generates a clutter with altitudes, the joint density ( $f(x, y)$ ) will be considered.

Table 5. Correlation between latitude, longitude, and altitude in a medium clutter density environment.

Correlation (r)	Latitude	Longitude	Altitude
Latitude	1	0.03976921	0.35365983
Longitude	0.03976921	1	-0.04997897
Altitude	0.35365983	-0.04997897	1

Figure 12 shows the scatter plots of all the variables. One can find that there exists a slightly positive correlation between altitude and latitude, meaning that as an altitude value grows, the latitude value also increases. Therefore, the joint density will be considered, when simulating clutter along with altitude information.

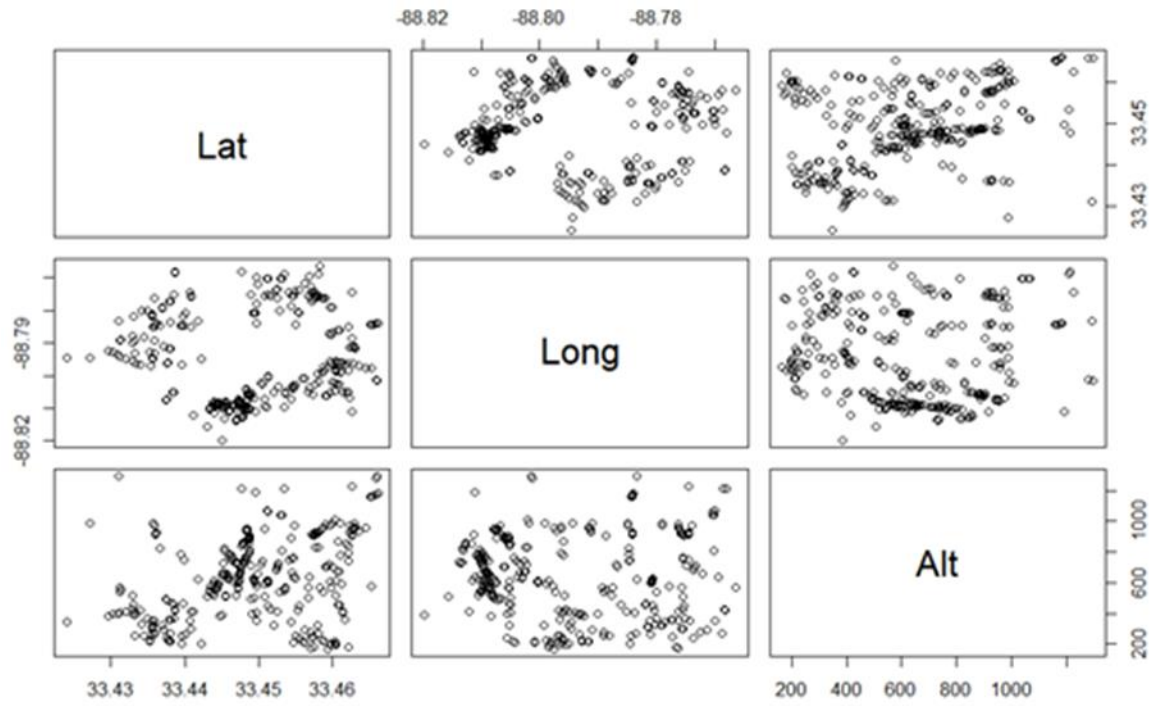


Figure 12. Scatter plots in a medium clutter density environment.

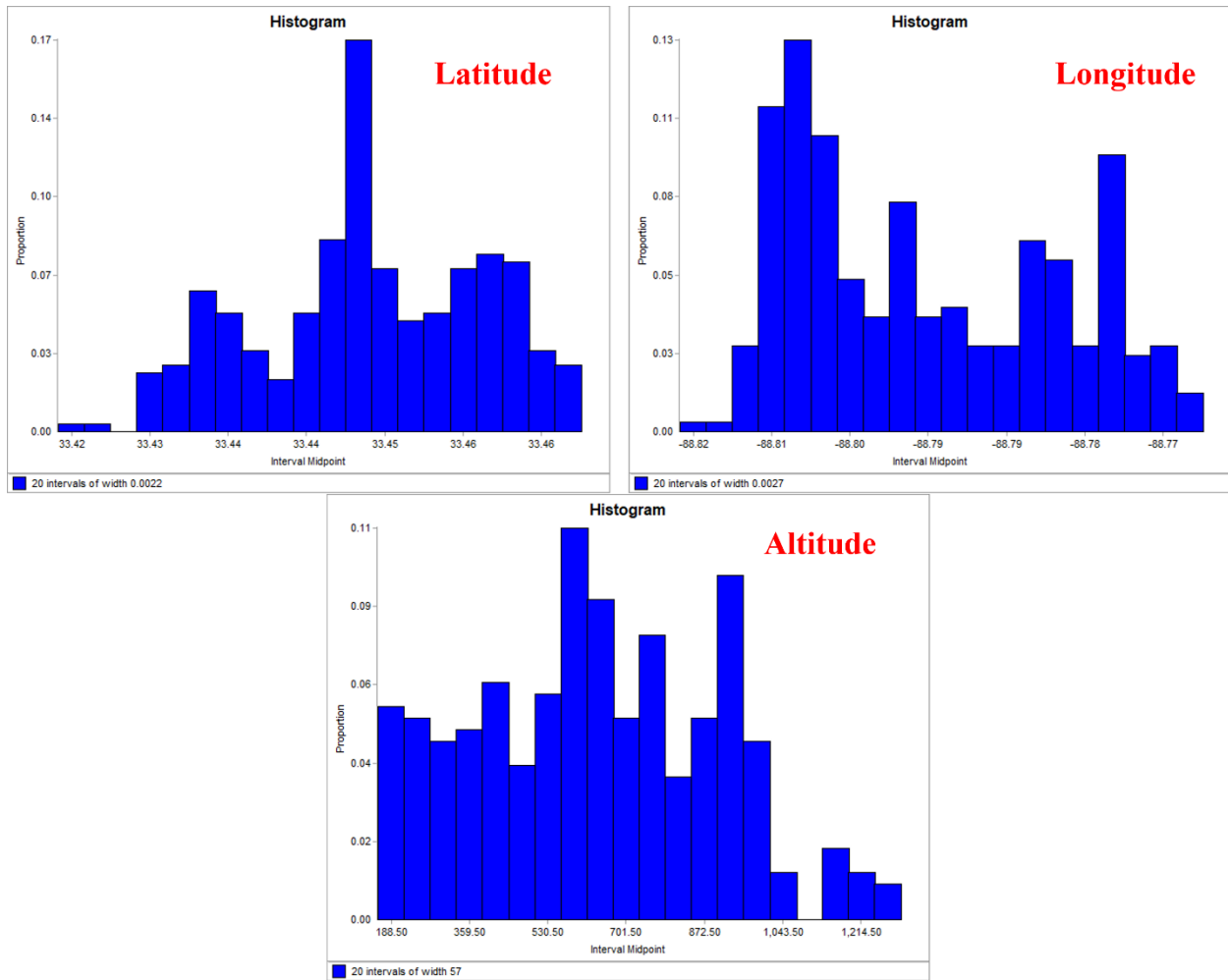


Figure 13. Histograms of latitude, longitude, and altitude in a medium clutter density environment.

To simulate the clutter in a medium-clutter density environment, the team selected 22 well-known distributions, and they were fitted; however, none of the distributions were significant enough to demonstrate any of those three variables. As shown in Figure 13, none of the three histograms show any specific patterns matching any known distributions. Therefore, the researchers decided to find empirical CDFs of all three variables to simulate them.

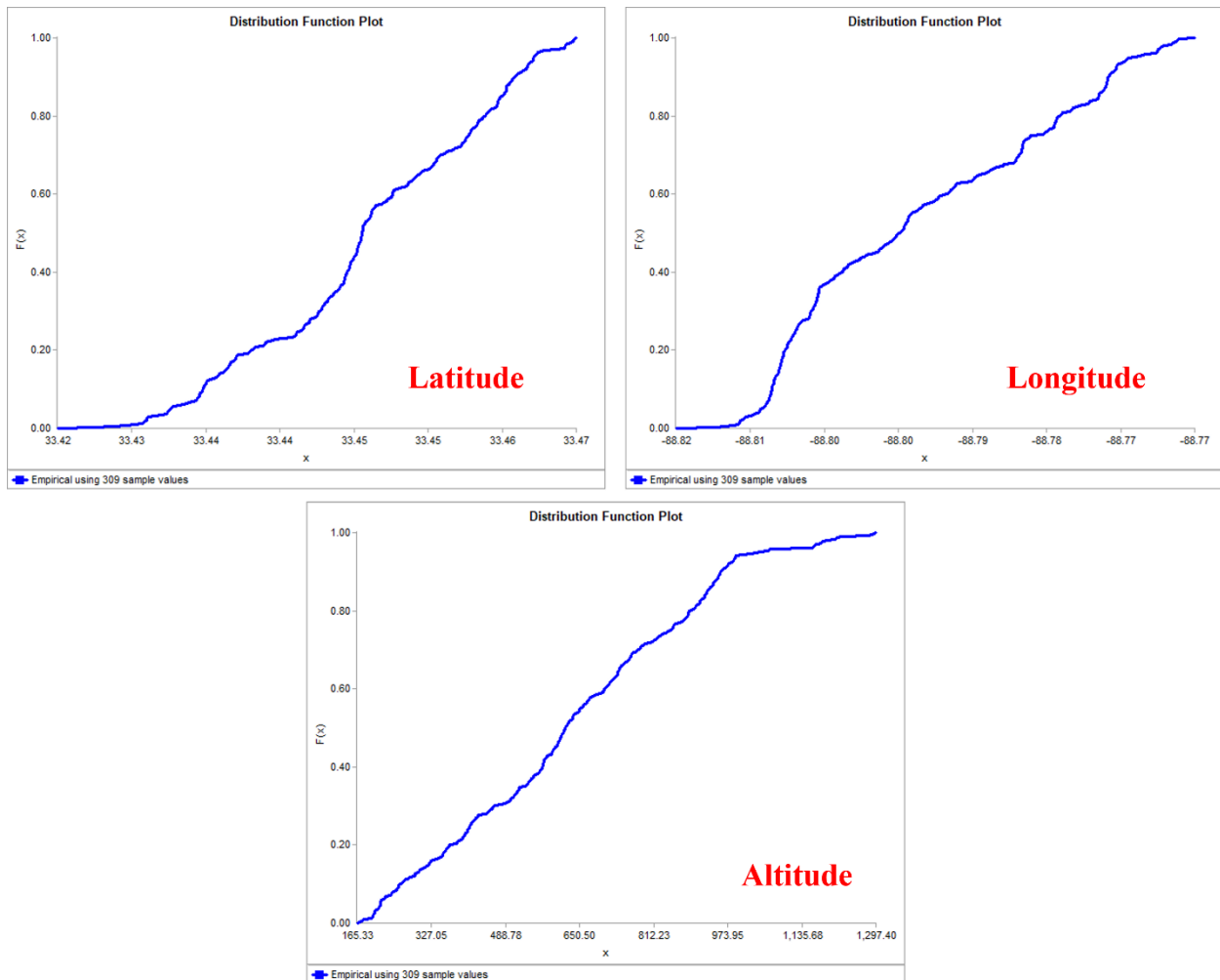


Figure 14. The cumulative density function of latitude, longitude, and altitude in a medium clutter density environment.

The three images in Figure 14 show three CDFs for all three variables. Using all the CDFs as well as reverse mapping described in Algorithm 1, the team successfully simulated clutters in a medium clutter density environment, as shown in Figure 15. It is found that the relative frequency is well incorporated in the simulated clutter. The same approach has been applied to the last configuration (low-level density environment).

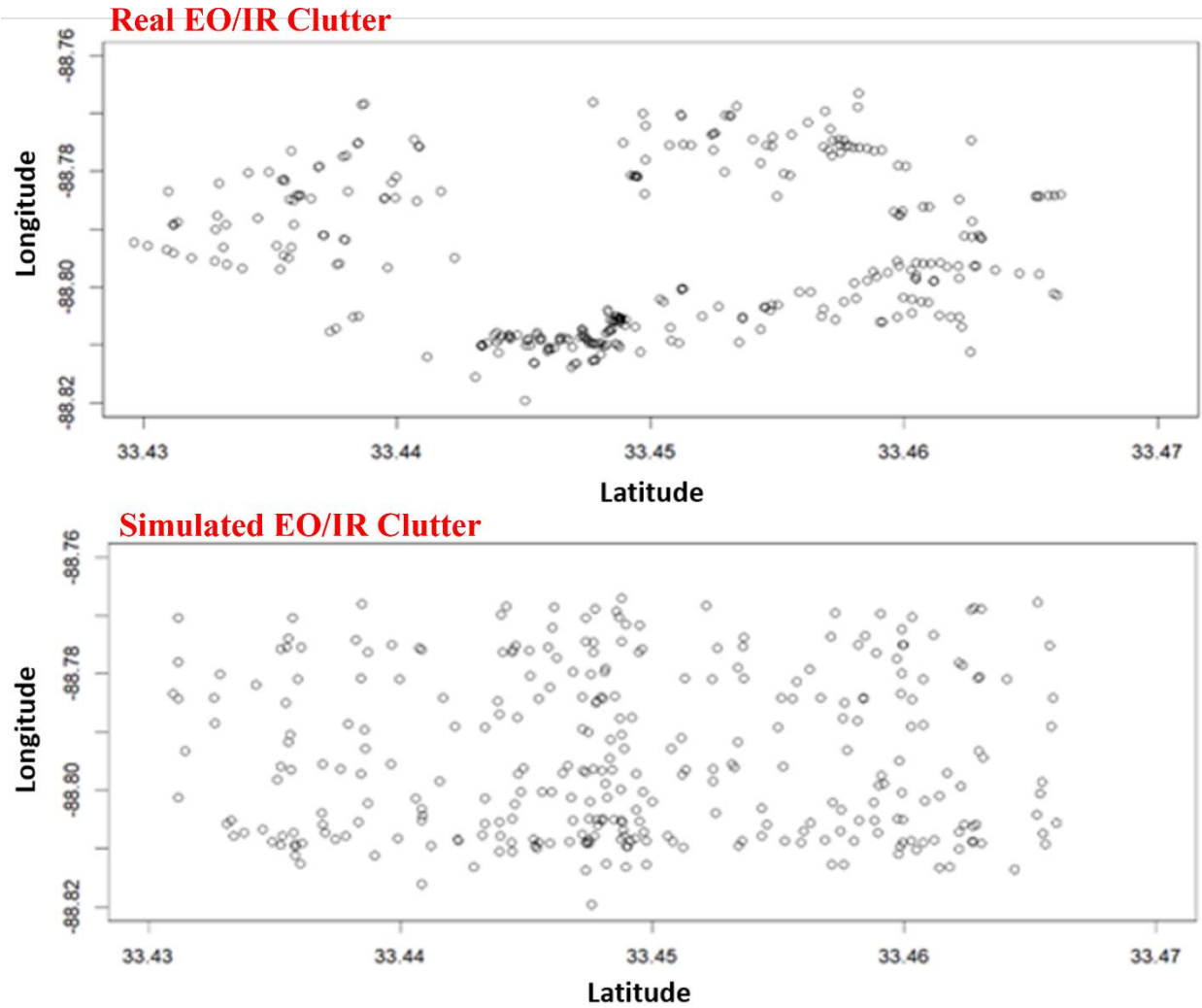


Figure 15. Real EO/IR clutter vs Simulated EO/IR clutter in a medium clutter density environment.

### 2.3.4 Case 3: Low

Since it is required to check whether any significant correlations are observed before clutter simulation, researchers checked the correlation values. Interestingly, As Table 6 shows, a significant positive correlation between latitude and longitude is observed (0.48). Moreover, the altitude is correlated with both latitude and longitude, which implies that all the joint densities ( $f(x, y), f(x, z), f(y, z)$ ) should be considered.

Table 6. Correlation between latitude, longitude, and altitude in a low clutter density environment.

Correlation (r)	Latitude	Longitude	Altitude
Latitude	1	0.4800939	0.1673565
Longitude	0.4800939	1	0.3086017
Altitude	0.1673565	0.3086017	1

To have a better understanding of all three correlations, all the scatter plots are developed in Figure 16. The positive correlations are observed in all three pairs, so all three joint densities should be derived. Moreover, it is also found that the altitudes between 200 and 400 and longitudes between -88.78 and -88.77 are omitted, which were excluded in pre-processing. Those points were not considered clutters but the results of the aircraft operations.

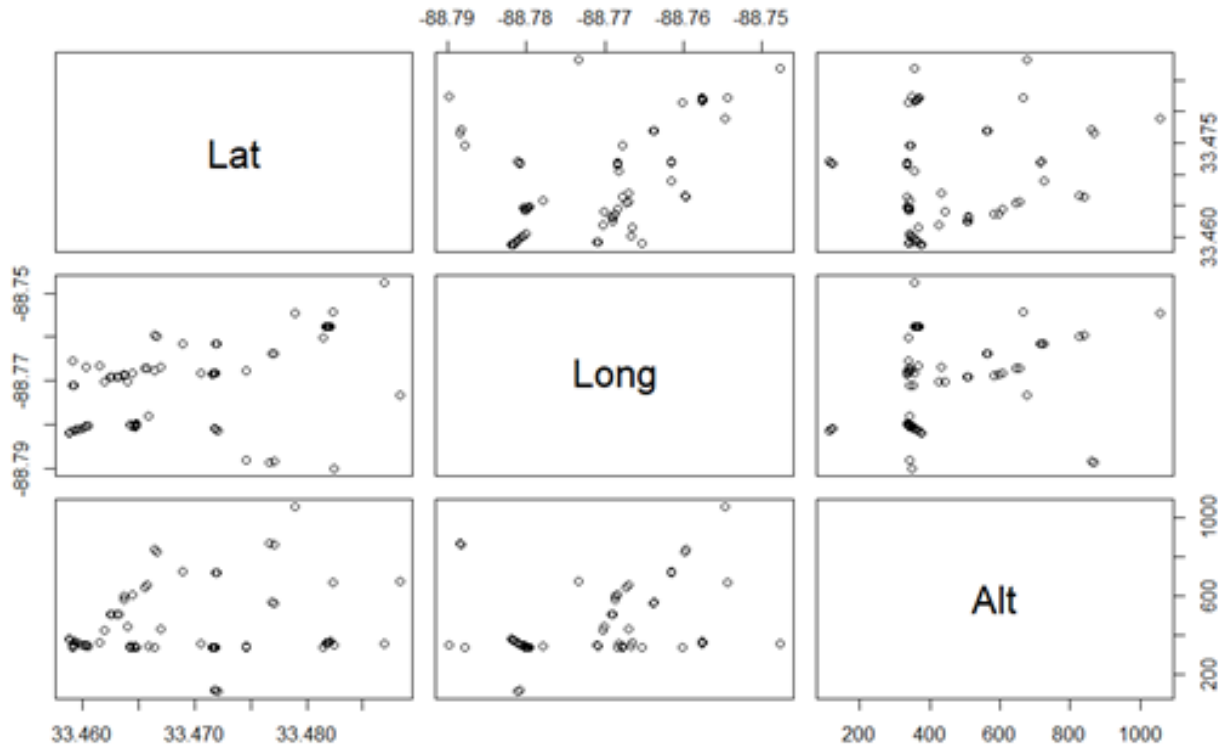


Figure 16. Scatter plots in low clutter density environment.

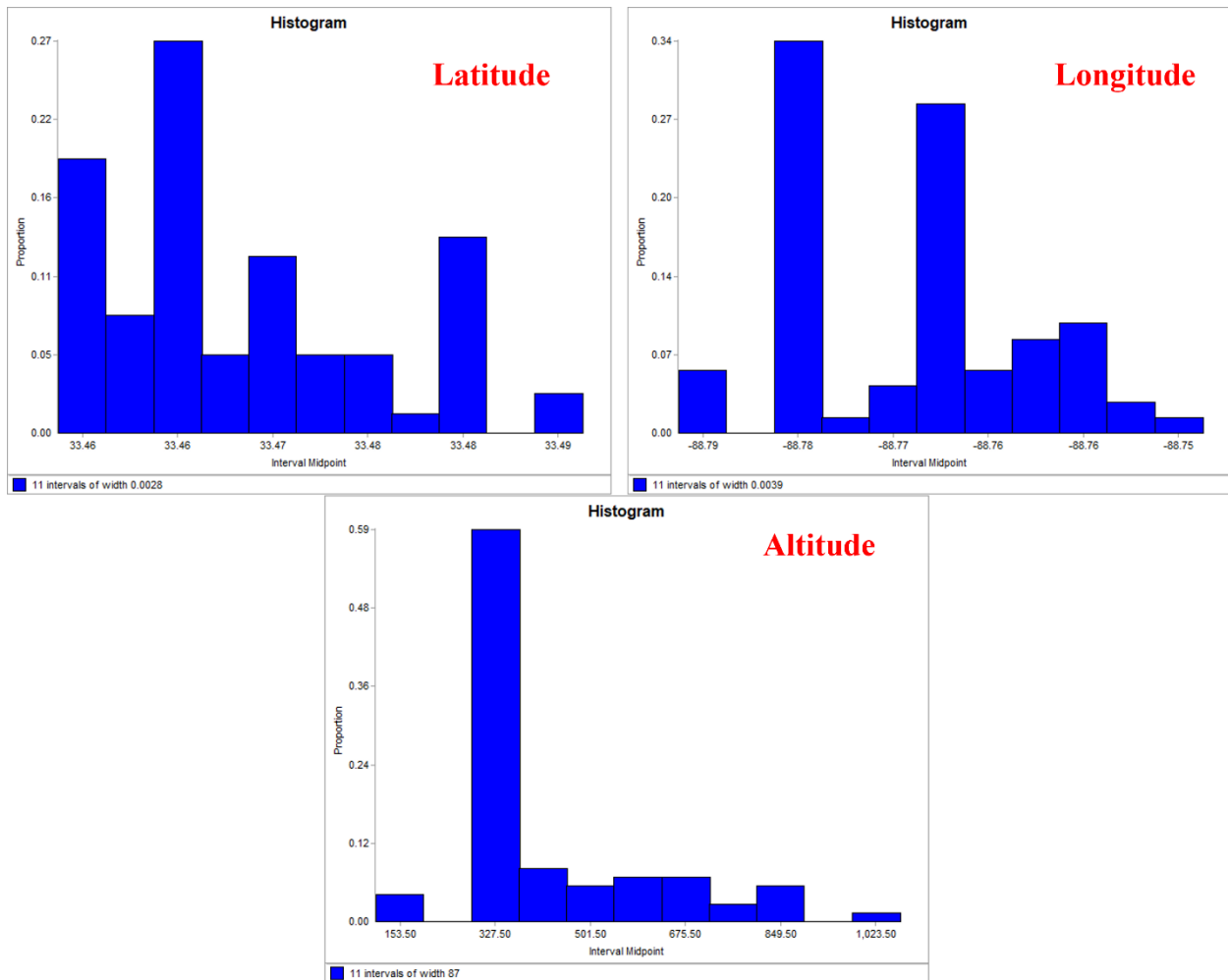


Figure 17. Histograms of latitude, longitude, and altitude in a low clutter density environment.

To simulate the clutter in a low-clutter density environment, the team selected 22 well-known distributions in high- and low-clutter density environments. As shown in Figure 17, none of the distributions were significant enough to demonstrate any of those three variables, meaning that none of them matched any known distributions' probability density functions. Therefore, the team decided to find empirical CDFs of all three variables to simulate them, as shown in Figure 18.

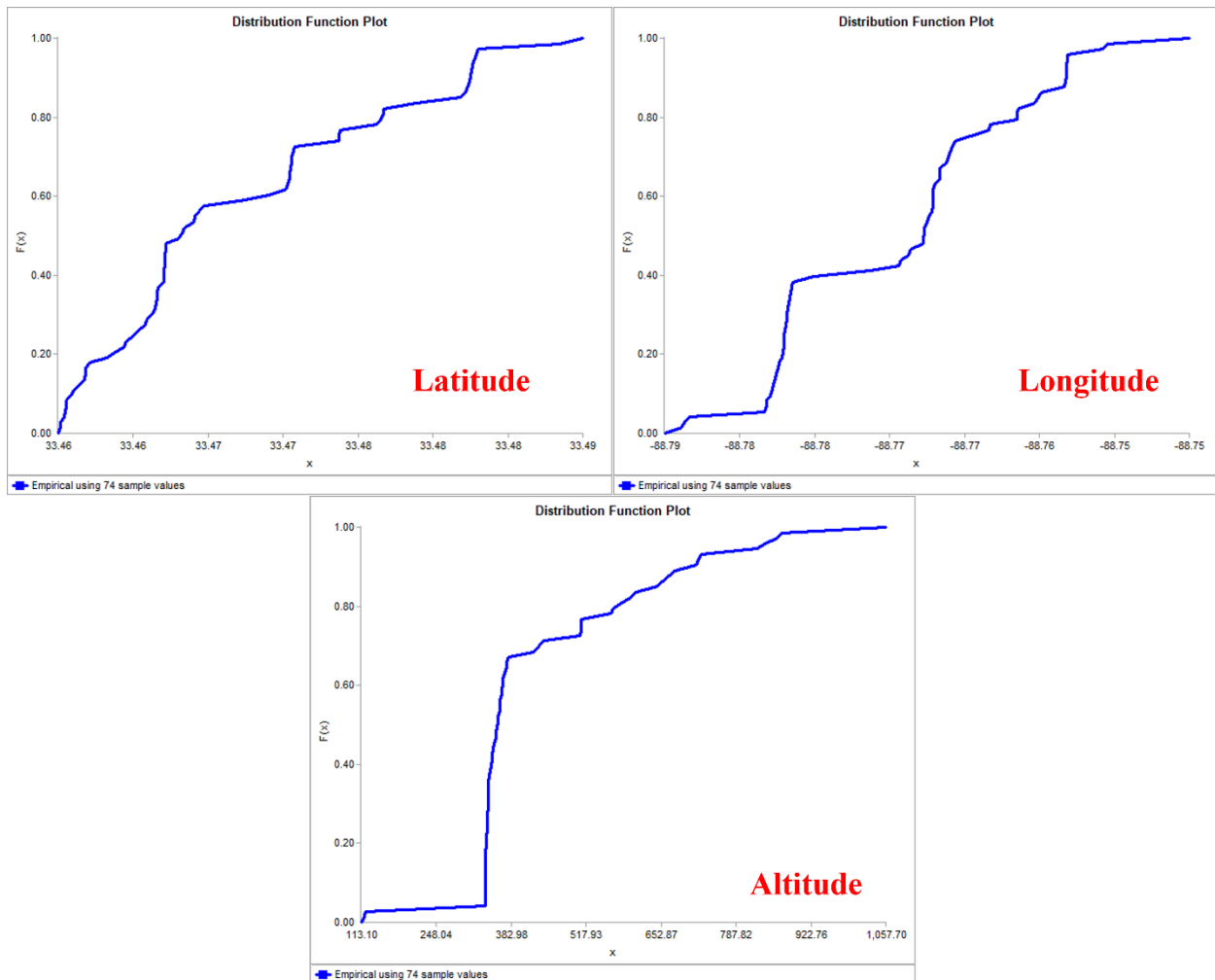


Figure 18. The cumulative density function of latitude, longitude, and altitude in a low clutter density environment.

The three images in Figure 18 show three CDFs for all three variables. Using all the CDFs as well as reverse mapping described in Algorithm 1, the researchers simulated clutters in a lower clutter density environment, as shown in Figure 19. In this simulation, the joint density has not been considered yet. The researchers identified it as a future work: the team will incorporate all the joint densities and simulate the clutters in a low clutter density environment.

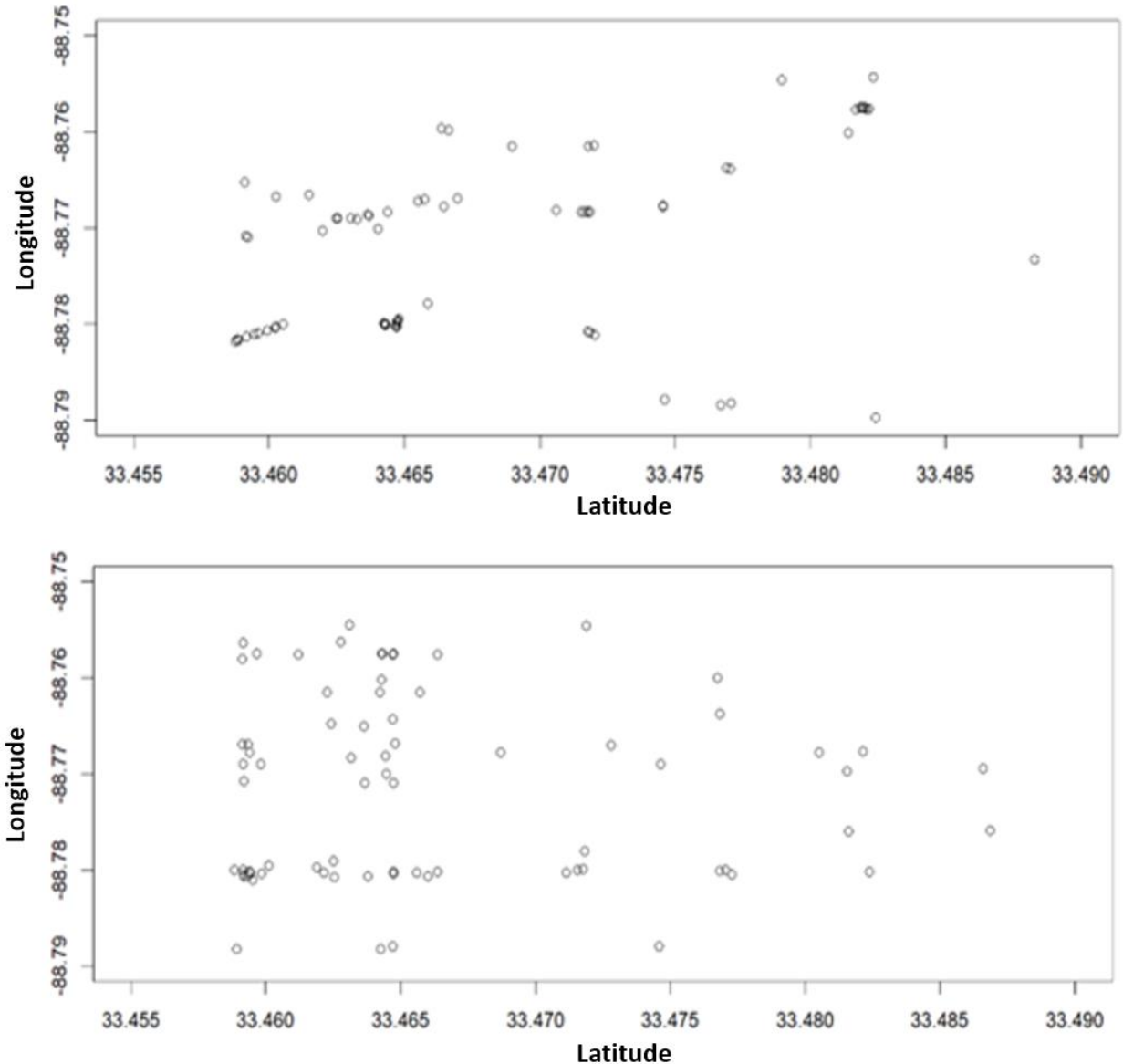


Figure 19. Real EO/IR clutter vs Simulated EO/IR clutter in a medium clutter density environment.

Future work will include incorporation of trajectories using stochastic modeling. The team will include trajectories of the clutter using Stochastic models- such as Brownian Motion. The following tentative algorithms will be applied:

**Step 1. Define the Parameters:**

Initial positions ( $x_0, y_0, z_0$ ) are selected from the initialized distribution.

Diffusion coefficient (D): A constant related to the magnitude of randomness in the motion. Another way to call it is “drift.” Researchers will calculate average drift using all the trajectories.

**Step 2. Generate Random Displacements:**

Brownian motion involves adding random displacements to the current position at each time step. The displacements will be drawn from a normal distribution with mean zero and variance  $(2 \times D \times \Delta t)$ . One can use a random number generator for this purpose. The random displacements can be generated as follows:

**2.1** Generate two random numbers  $\Delta x$  &  $\Delta y$  , which are sampled from the empirical distribution of the collected  $\Delta x$ ,  $\Delta y$

**2.2** Update the position at each time step:

$$x(t + \Delta t) = x(t) + \Delta x , y(t + \Delta t) = y(t) + \Delta y$$

**Step 3. Repeat for Multiple Time Steps:** Continue updating the position of the object as researchers reach to the enough steps as needed. The distribution of all the simulated trajectory lengths will be the same as the empirical distribution of real trajectory lengths.

Completion of implementing and applying algorithms will generate enough trajectories, capturing dynamic behaviors of clutters in the observed area.

## **2.4 Data Modeling and Synthetic Dataset Generation**

### **Step 1: Clean data.**

The field data was collected at various sites to vary the rate and density of clutter. A few steps were taken to ensure that the only data digested by the following process was clutter data. First, a description of some of the nuances of the EO/IR Ground-based DAA system was discussed. The DAA system used attempts to classify the detected intruders as birds, drones, crewed aircraft, or other more specific classes. The team, through experience operating and analyzing the system's performance, determined that a few filters were necessary to ensure that only clutter data was fed into the simulated clutter generator. The first filter removed any data where the researchers knew a crewed aircraft was present within the surveillance volume of the system. This usually occurred with data that was taken from field tests for various ASSURE and related projects. The second filter then removed any classification of "BIRD" as those alerts would be removed in standard operations. The remaining clutter data then had only detections and tracks for alerts that threatened the safety of the operation, while still including tracks of fixed-wing aircraft, rotorcraft, or other aircraft that were not explicitly identified as crewed. It should be noted, that in real-world systems, misclassifications of birds as aircraft may still occur, and such cases would not necessarily be removed by the system. As described earlier, three representative datasets were selected for processing. These datasets range from the lowest observed clutter rate, defined as clutter tracks per hour, to the highest observed clutter rate.

### **Step 2: Characterize data.**

Once the data was appropriately filtered, researchers characterized the behavior of the clutter data. Various approaches were used to understand the relationships between elements. The final approach used simple distributions of range from sensor, altitude, and velocities. The data had the following characteristics. The following cartesian coordinate system is used for the following

described dataset:  $\mathbf{X}$  represents the north-to-south position of each track,  $\mathbf{Z}$  represents the east-to-west position of each track, and  $\mathbf{Y}$  represents the vertical position of each track.

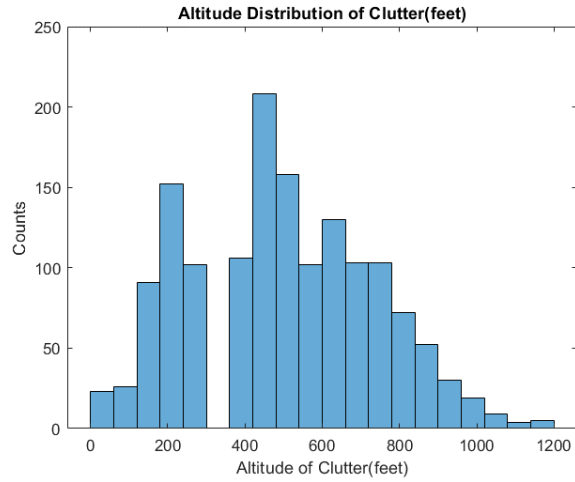


Figure 20. Altitude distribution of single clutter dataset, in feet.

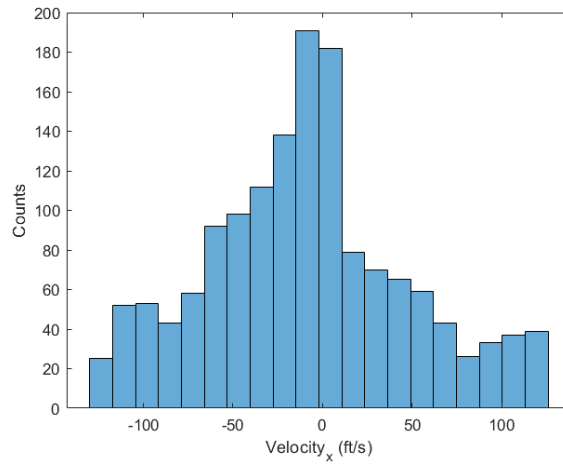


Figure 21. Velocity in x-direction (horizontal) for clutter data, in feet per second.

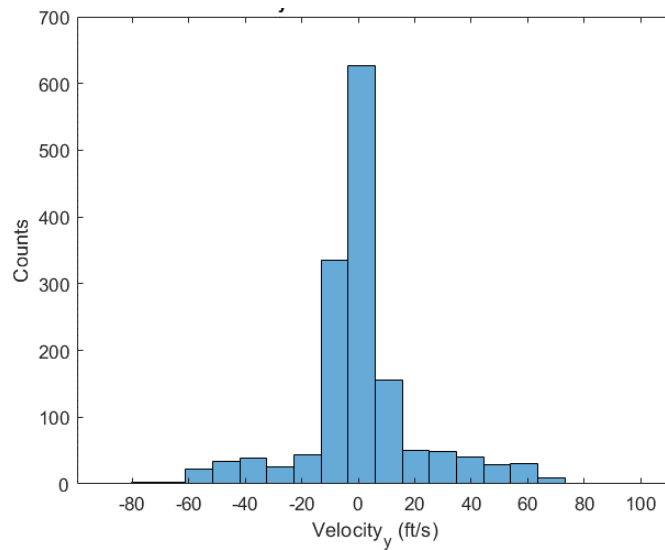


Figure 22. Velocity in y-direction (horizontal) for clutter data, in feet per second.

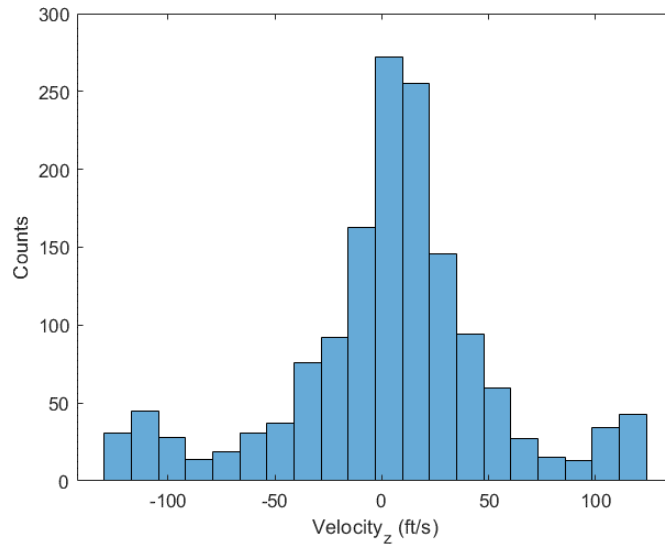


Figure 23. Velocity in z-direction (vertical) for clutter data, in feet per second.

### Step 3: Initiate a point

Once the distributions of the dataset were understood, the first step in forming new clutter tracks was the initialization of a point in x-y-z space. The range from sensor distribution influenced a variable,  $r$ , that would be used with a relative angle between the simulated clutter's initial state, and the sensor's north heading. The research team determined, through experience, that the angle at which clutter occurred was dependent on the presence of physical objects detected during field data collection. One major assumption of the simulated clutter dataset is that, for convenience, there is assumed to be a uniform possibility of a clutter track initiating anywhere within the surveillance volume but constrained by the range from sensor distribution.

Therefore, a single clutter track was determined by selecting a random range from the range from the sensor distribution, selecting a random angle from a uniform distribution from 0 to 360, selecting a random altitude from the altitude distribution, and then converting to an x-y-z Cartesian coordinate.

$$x = r_{fromSensor} * \cos(\alpha)$$

$$y = r_{fromSensor} * \sin(\alpha)$$

$$z = altitude$$

Finally, researchers determined that the length of the track for each field data clutter track could be used to interpolate each clutter track. Kinematic equations were used to extrapolate a single initial data point to a track with a representative length as determined by randomly selected values from the length of track distribution.

The following data was sent to the next steps within the process.

$$State_{clutter}(1) = [t \ x \ y \ z]$$

In the above, t is the length of the track, and [x y z] represent the initial position of the clutter track.

The process then takes representative velocities in the x, y, and z directions and attaches them to the initial state vector for a clutter track. This further expands the initial state as below:

$$State_{clutter}(1) = [t \ x \ y \ z \ V_x \ V_y \ V_z]$$

#### Step 4: Interpolate

Researchers kinematically interpolated the initial state vector for the length of track, t. Researchers determined that assuming zero acceleration, while convenient, did not produce tracks that appeared to behave like the field data. Researchers added a small acceleration based on a normal distribution in the horizontal and added a small vertical acceleration based on a normal distribution. The resulting simulated dataset appeared more realistic as a product of the small acceleration.

#### Step 5: Expand to a larger area

As the intent of the clutter data collection and analysis process is to simulate the effect of clutter on UAS attempting to avoid crewed aircraft, the dataset needed to be expanded to a wider area. While the sensor had a one-and-a-half nautical mile range at best, the encounter set spanned up to 10 miles horizontally. To use this simulated data, the approach needed to produce a larger area of clutter data. To do this, researchers assumed there were 25 evenly distributed sensors across a 10 by 10 nautical mile volume. The approach for simulating data was then repeated 25 times for each unique sensor location for 30 minutes of simulated data and produced the following result.

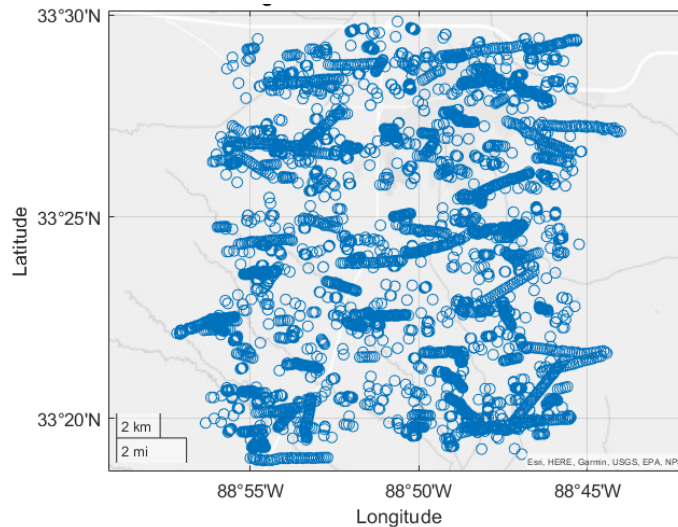
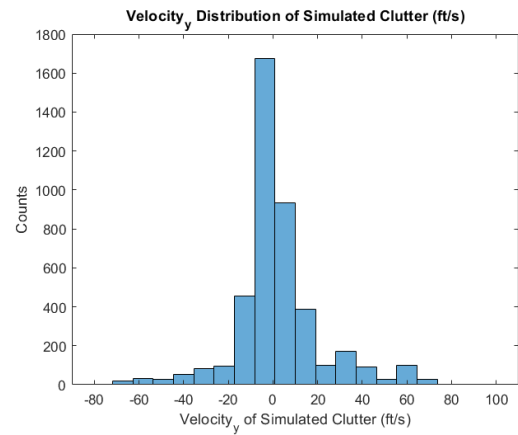
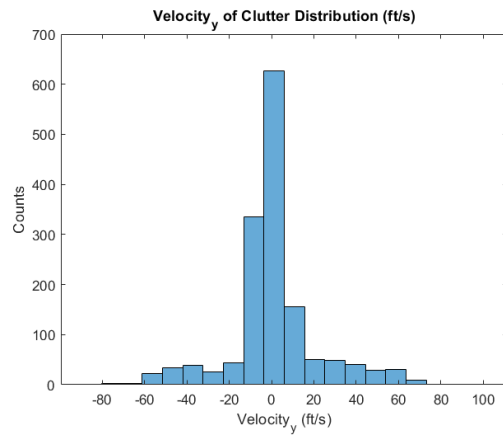
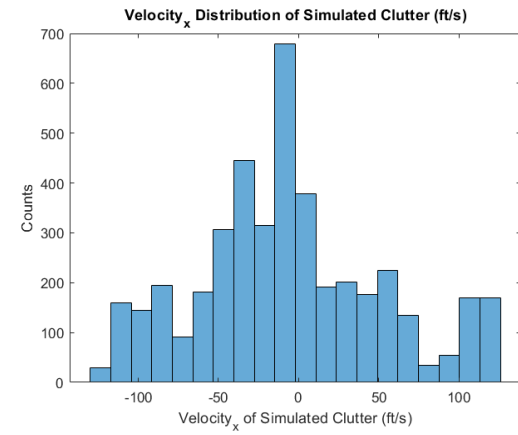
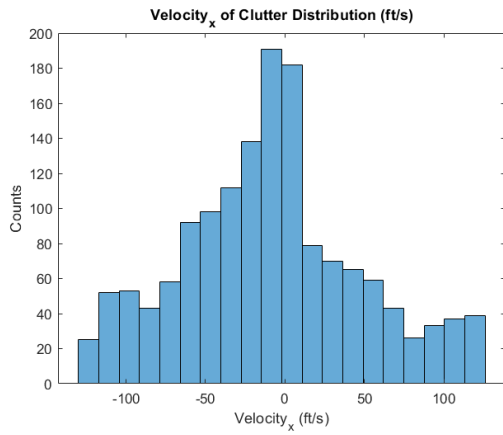
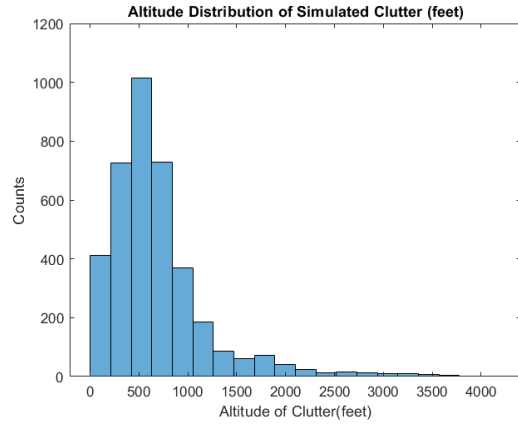
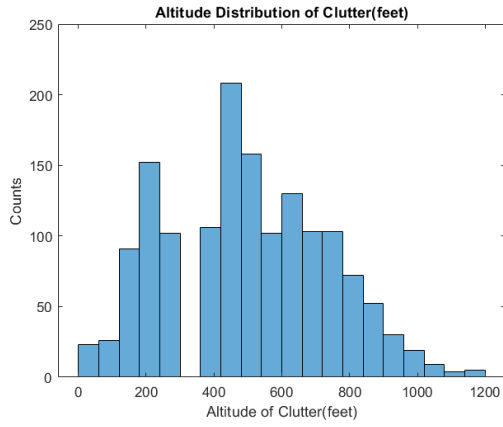


Figure 24. Resulting wider area of clutter data, with 30-minute length.

#### Step 6: Compare back

Researchers then compared the distributions of the real data versus the simulated data. The following charts visualize the likeness of the two datasets. Since the simulated data covered 25 times the area of the field data, the distribution formed with a much larger dataset.



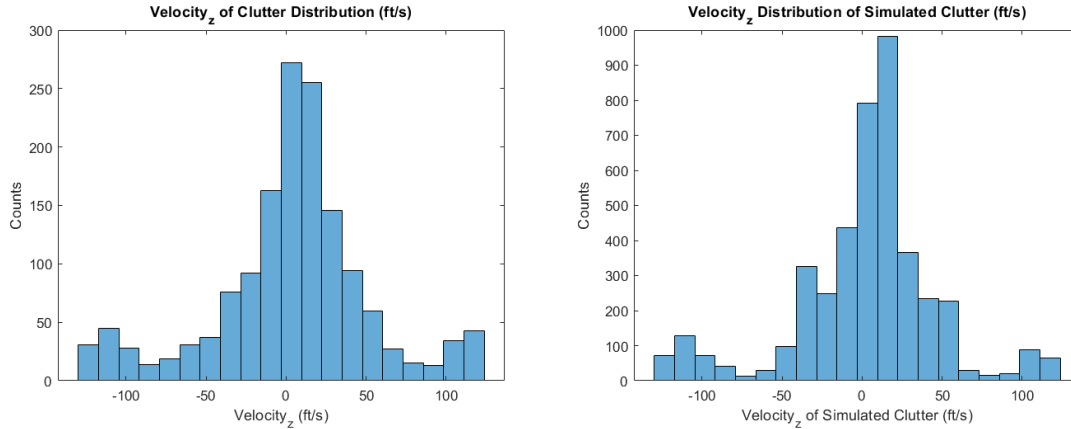


Figure 25. Various distribution comparisons of field data (left) and simulated data (right).

The synthetic clutter was then passed along to the A57 simulation team for fast-time encounter simulations to understand the modeled clutter’s effect on operational suitability and safety.

### 3 ENROUTE MODELING AND SIMULATION RESULTS

#### 3.1 Simulation Setup

The encounters used for this task are drawn from the Glendale Hub-and-Spoke encounters [OPVAL]. These encounters feature an ownship vehicle simulating a package delivery, together with an intruder vehicle trajectory obtained from actual ADS-B traffic observed in the NAS and provided by the TCAS Program Office and MITRE. 20,000 unique ownship vehicle trajectories radiate at 20-40 kts from a warehouse in Glendale, CA, at uniform headings from 0 to 359 degrees, and a set of 26,845 ADS-B intruder trajectories are paired with them to form a total of 1,000,000 encounters that include take-off, enroute flight, and landing. The reduced set of roughly 665,000 encounters only included the enroute portion and removal of some duplication. The reduced set was used for this effort.

Initial simulations of all 665,120 encounters were performed resulting in approximately 12,000 alerting encounters. About 2,000 of these alerted within the first five seconds and were discarded. An additional 10,000 non-alerting encounters were chosen at random, resulting in a *total of 20,000 encounters* used in the following analysis.

#### 3.2 Ground Based Radar Results

##### 3.2.1 Safety Analysis: Nominally Alerting Encounters

The safety analysis in Table 7 revealed the unexpected result that the total number of LoWC was *reduced* when clutter was added to the one-on-one encounters. As noted previously, the reduction in LoWC is an artifact of the simulation setup in which the ownship was biased towards an encounter, so any motion induced by clutter would have the net effect of reducing the likelihood of encountering the original intruder. This should be considered when architecting DAA simulations as it has a first-order effect on the resulting safety statistics and airspace usability assessments. In the table, the notation used are:

No DAA: Unmitigated (ownship **does not** follow sXu guidance)

With DAA: Mitigated (ownship **does** follow sXu guidance)

OpVal: ACAS sXu Operational Validation Report (Sept 2022)

Results: Current CAL Results

Target: Target Safety Value

Table 7. Analysis for varying levels of clutter. (Note, reduction in safety statistics are due to likely simulation bias as noted in Section 3.2.1)

Clutter Flux Density (False tracks/nm <sup>2</sup> -hr)	Alerting Encounters	LoWC (with DAA/ no DAA)	NMAC (with DAA/ no DAA)	RR (LoWC)	RR (NMAC)	P(LoWC)	P(NMAC)	SLoWC (mean)	SLoWC (>33%)
				OpVal					
				Results					
				Target					
None	9791	259/2879	1/224	0.0900	0.0045	0.0254	9.8e-5	8.55	0.00130
				0.0235	0.0045				
				0.4000	0.1800				
47	10092	242/2879	2/224	0.0841	0.0089	0.0238	1.9e-4	8.36	0.00110
79	10145	238/2879	1/224	0.0827	0.0045	0.0234	9.8e-5	8.56	0.00098
106	10171	189/2879	0/224	0.0656	0	0.0186	0	9.26	0.00110
260	10176	170/2879	1/224	0.0590	0	0.0167	9.8e-5	10.17	0.00120

Table 8. LoWC changes based on levels of clutter.(Note, reduction in safety statistics are due to likely simulation bias as noted in 3.2.1)

Clutter Flux Density (False tracks/nm <sup>2</sup> -hr)	Alerts	LoWC (with DAA/ no DAA)	LoWC Subtracted from Nominal	LoWC Added to Nominal	Net change
None	9791	259/2879	-	-	
47	10092	242/2879	158	141	-17
79	10145	238/2879	178	157	-21
106	10171	189/2879	202	132	-70
260	10176	170/2879	207	118	-89

For this clutter set, total number of LoWCs are *reduced* as more clutter is added. Some LoWCs are added, but more are subtracted, thus the observed *net* reduction in LoWC with the addition of clutter, as shown in Figure 26. Consider introducing the discussion here about the simulation bias and that this is not believed to be a real effect but an artifact of the simulation setup that is biased

towards creating encounters. Alternatively, mention that the reduction in LoWC will be discussed later and that these results are believed to be a simulation artifact.

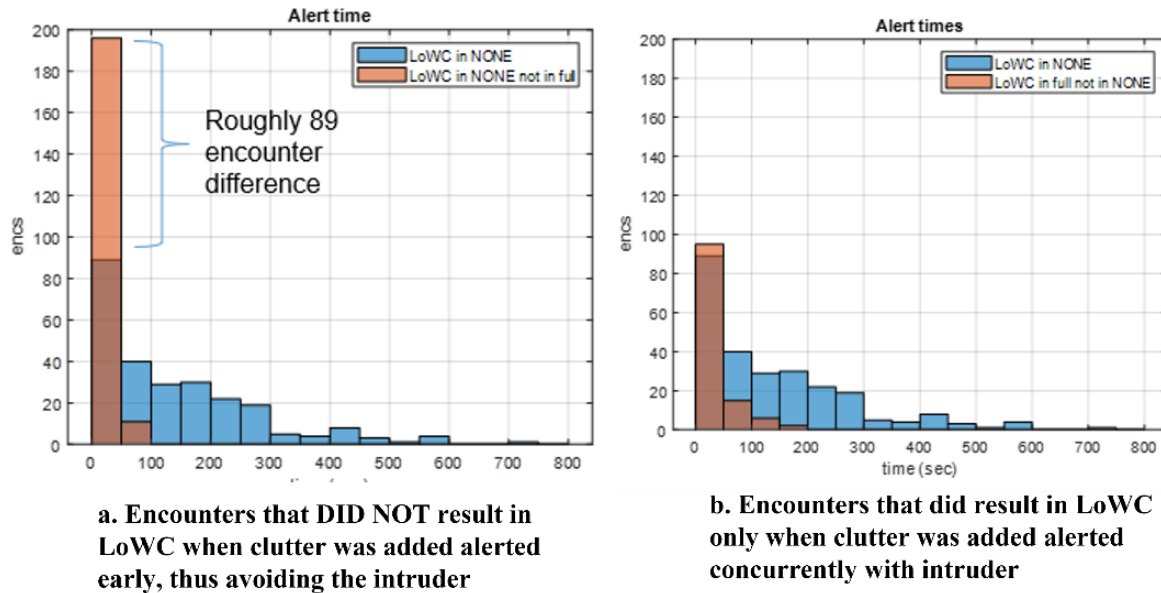


Figure 26. Histogram showing differences in LoWC with and without Clutter. Chart on the right indicates that LoWC is due to early alerting and diverting of the ownship. When a delay to alert only when in proximity to the intruder (figure on the right), the LoWC rates better align with the intruder-only data sets.

LoWCs reduce with more clutter likely because:

1. Particular clutter tracks are relatively short-lived (order of tens of seconds), so likely to cause alerts but NOT LoWC,
2. Encounters are set up such that an intruder is likely to cause an alert, and
3. Increased clutter causes the ownship to maneuver away from the intruder sooner than it would otherwise, and there's no effort to return to course.

To address item 3, one needs to show that RA's issued against clutter mostly happen *before* an alert would have occurred against the intruder, thus causing the ownship to maneuver in a random direction with respect to the intruder.

### 3.2.2 Safety Analysis: 10K Nominally Alerting Encounters

The LoWC/NMAC analysis was applied to the *clutter* as though the clutter tracks represented real vehicles. This was done only as an exercise to demonstrate the increased track density in the airspace. The LoWC/NMAC statistics in the two right-most columns of Tables 9-10 do not represent safety statistics as typically defined but were computed to aid in understanding the conditions in the airspace.

Table 9. Analysis including treatment of clutter as ‘Real’ tracks. (Note, reduction in safety statistics are due to likely simulation bias as noted in Section 3.2.1)

Clutter Flux Density (False tracks/nm <sup>2</sup> -hr)	Alerting Encounters	Ownship+intruder encounter statistics		Ownship+intruder+clutter encounter statistics (Clutter treated as “real” vehicle)	
		LoWC (with DAA/no DAA)	NMAC (with DAA/no DAA)	LoWC (with DAA/no DAA)	NMAC (with DAA/no DAA)
None	9791	259/2879	1/224		
47	10092	242/2879	2/224	1581/3937/	62/288
79	10145	238/2879	1/224	2784/5472	109/424
106	10171	189/2879	0/224	4260/7420	123/605
260	10176	170/2879	1/224	6262/8621	138/822

Table 10. Analysis including treatment of clutter as ‘Real’ tracks in percentage. (Note, reduction in safety statistics are due to likely simulation bias as noted in Section 3.2.1)

Clutter Flux Density (False tracks/nm <sup>2</sup> -hr)	Alerting Encounters	Ownship+intruder encounter statistics		Ownship+intruder+clutter encounter statistics (Clutter treated as “real” vehicle)	
		LoWC (%)	NMAC(%)	LoWC	NMAC
None	9791	9	0.4	-	-
47	10092	8.4	0.9	40.2	21.5
79	10145	8.2	0.4	50.9	25.7
106	10171	6.6	0	57.4	20.3
260	10176	5.9	0.4	72.6	16.8

### 3.2.3 Non-alerting encounters, Full Clutter

Discussions regarding the early alert conjecture included reference to the fact that the intruder encounters under study were pre-disposed to alerts leading to ‘encounter bias.’ This effect may cause any early maneuver (due to clutter and before ownship-vs-intruder interaction) to inadvertently appear to increase safety by steering the ownship away from the intruder prematurely in the simulation. To further investigate this, the results in Table 11 show the results for intruders that were not on a conflict trajectory

with the drone. No DAA alerts occur when there is no clutter because aircraft are not on trajectories that would create a conflict. However, when clutter is added to the simulation, the clutter results in a DAA alert causing the drone to avoid the clutter which on occasion induces an encounter with the intruder aircraft. A significant percentage increase in LoWC is noted. Table 11. Analysis using 65K non-alerting encounters.

Clutter Flux Density (False tracks/nm <sup>2</sup> -hr)	Alerting Encounters	Ownship+intruder encounter statistics		Ownship+intruder+clutter encounter statistics (Clutter treated as “real” vehicle)	
		LoWC (with DAA)	NMAC (with DAA)	LoWC (with DAA)	NMAC (with DAA)
None	0	0	0	-	-
260	38100	9	1	8731	216

Note that when intruders are not on a conflicting trajectory with the drone and there is no clutter, no LoWC or NMAC events occur. However, when clutter is introduced a significant increase in LoWC and NMAC events occur with intruder aircraft. LoWC goes from zero to 9 events which is more than a 900% (or 9x) increase. What is even more striking is the number of LoWC events with intruders and clutter tracks that are treated as aircraft. The perceived LoWC events rises to 8,731. Both a significant increase in real NMAC events (x9) that increases the potential for a mid-air collision and an even greater increase in perceived NMAC events (x8731) many of which are illusionary and increase operational burdens occurs due to the introduction of clutter.

### 3.2.4 Delayed clutter

Discussions regarding the decrease in LoWC once the Ground Based Radar (GBR) clutter was introduced lead to the conjecture that early alerts by the clutter tracks were precluding the ownship vs. intruder encounter. The simulation was modified, as shown in Figure 27, to mask the clutter traffic until *after* the ownship versus intruder alert commenced.

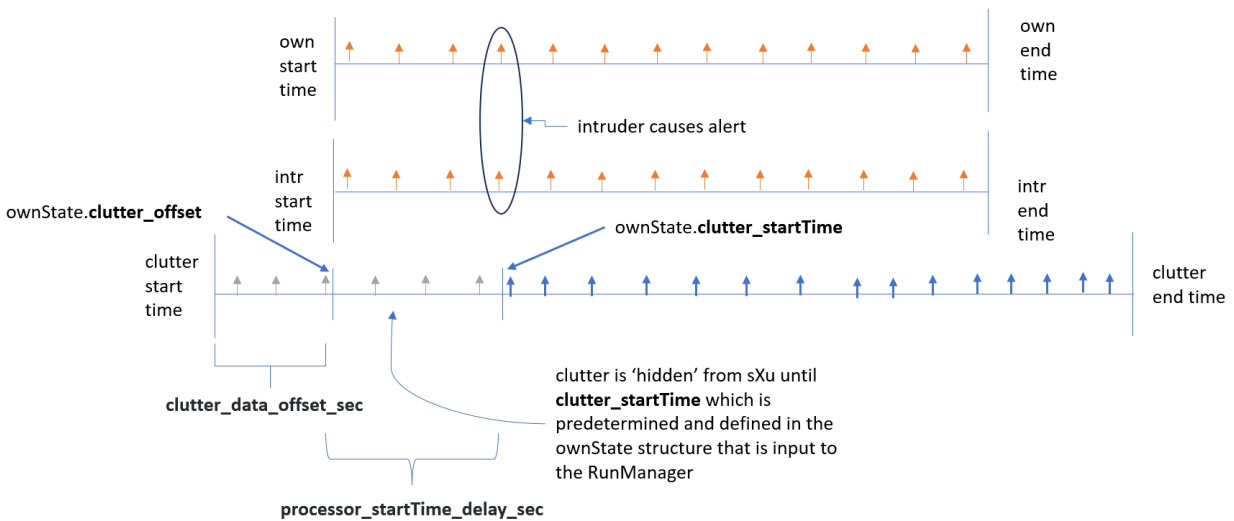


Figure 27. Modification to mask clutter until after intruder triggers alert.

Using this modified configuration, the conjecture of early alerting precluding the ownship versus intruder encounter was confirmed by the results shown in Table 12. That is, the number of LoWC increased with the addition of clutter so long as the ownship versus intruder alert happened to help compensate for the simulation artifacts and deficiencies discussed earlier. More work on this topic to improve clutter analysis in simulations is recommended as an area for future research.

Table 12. Results following simulation modification where clutter is hidden in the simulation until after there is an alert on the intruder aircraft.

Clutter Flux Density (False tracks/nm <sup>2</sup> -hr)	Intruder Alerting Encounters	Ownship+intruder encounter statistics		Ownship+intruder+clutter encounter statistics (Clutter treated as “real” vehicle)	
		LoWC (with DAA)	NMAC (with DAA)	LoWC (with DAA)	NMAC (with DAA)
None	9233	234	1	- N/A	-N/A
260	9206	318	1	3813	148

By comparing the top row with the bottom row when only considering events with real intruders, the introduction of clutter resulted in  $318/234 = 35\%$  more LoWC events. This indicates that the introduction of clutter had a significant impact on keeping aircraft separated. More data is needed to estimate the percent increase in NMAC events with intruders due to the introduction of clutter.

By examining the bottom row, the delayed clutter resulted in roughly  $3813/318 = 1,200\%$  (120x) more perceived LoWC events with the clutter than actually occurred with intruders. It also resulted in roughly  $14,800\%$  (148x) more reported NMAC events with the clutter than actually occurred with intruders. The addition of the clutter had a significant operational impact on the number of perceived and recorded events with most of the perceived events being illusory occurring with the clutter rather than an actual intruder.

The introduction of clutter resulted in a significant percentage increase in reduced separation events in the simulation as well as a much larger increase in perceived events and operational burden. More work on this topic to improve clutter analysis in simulations is recommended as an area for future research.

### 3.2.5 AGT Transition

Initial simulations of both the alerting and non-alerting encounter sets with clutter were configured such that the intruder aircraft utilized the ADS-B interface to ACAS sXu. Discussions with the ACAS development team concluded that the choice of using ADS-B as the interface for the intruder while using the Absolute Geodetic Track (AGT) interface for the clutter might affect the results, since the DAA algorithm would treat the intruder and the clutter traffic somewhat differently. To investigate this issue, the simulation was modified so that the intruder used the AGT interface as well, and the safety statistics were compared. Table 13 shows the comparison showing no significant difference in the results.

Table 13. Statistics using ADS-B vs AGT DAA interface for intruder.

Clutter Flux Density (False tracks/nm <sup>2</sup> -hr)	Alerting Encounters	LoWC (with DAA/ no DAA)	NMAC (with DAA/ no DAA)	RR (LoWC)	RR (NMAC)	P (LoWC)	P (NMAC)	SLoWC (mean)	SLoWC (>3%)
None ADS-B	9791	259/2879	1/224	0.0899	0.0045	0.0254	9.8e-5	8.55	0.00130
None AGT	9935	276/2879	0/224	0.0959	0	0.0271	0	7.73	0.00120
260 ADS-B	10176	170/2879	1/224	0.0590	0	0.0167	9.8e-5	10.17	0.00120
160 AGT	10177	169/2879	0/224	0.0587	0	0.0166	0	9.83	0.00110

### 3.2.6 Operational Suitability Analysis

Operational suitability analysis was performed on results using the alerting encounters together with the GBR clutter data. Figure 28 shows that increased clutter leads to a longer time spent in an alert state, but that time is split over multiple *separate* alerts.

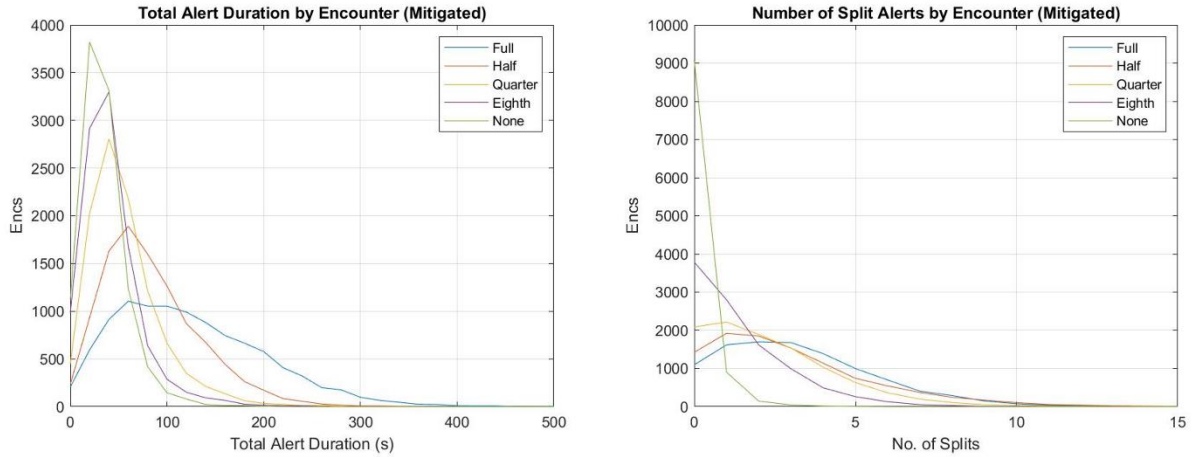


Figure 28. Total alert duration and number of split alerts per encounter.

The results in Figure 29 show that the varying clutter levels had only a small effect on the number of horizontal reversals per encounter and virtually no effect on the number of vertical reversals. Of note, in these figures, full clutter represents 260 targets/(nm<sup>2</sup>-hr) and the eighth represents 47 targets/(nm<sup>2</sup>-hr) appearing in the preceding tables.

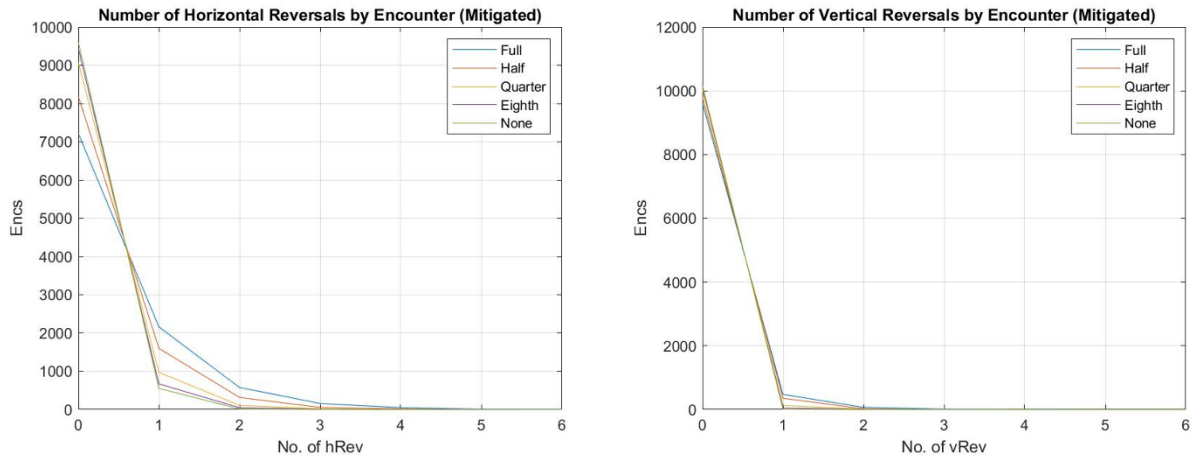


Figure 29. Number of reversals per encounter with varying levels of clutter.

### 3.3 EO/IR results

#### 3.3.1 MSU Variable Density Clutter

Three sets of clutter data were produced and injected into the simulation. Figures 30-32 show the overlay of the clutter data on the alerting encounter set.

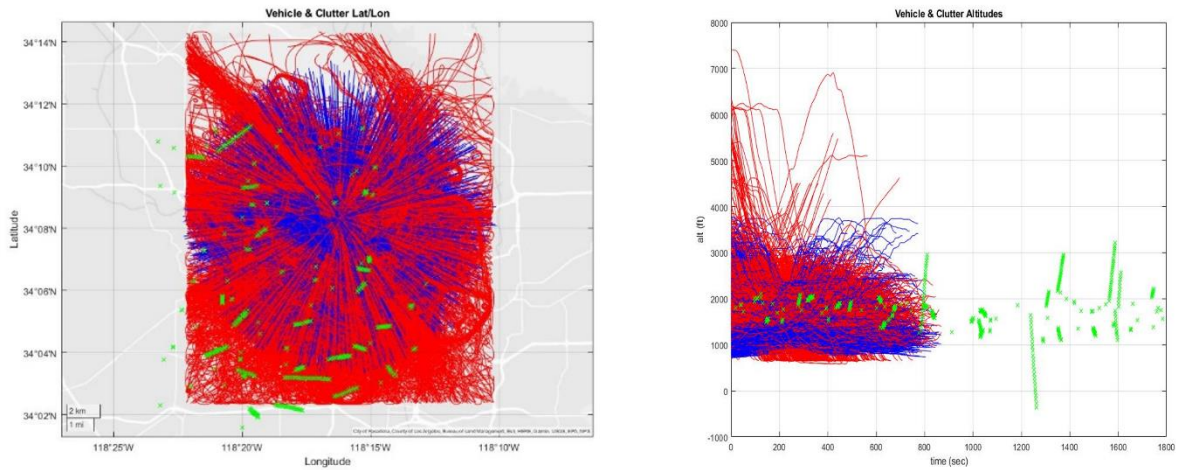


Figure 30. Low density clutter.

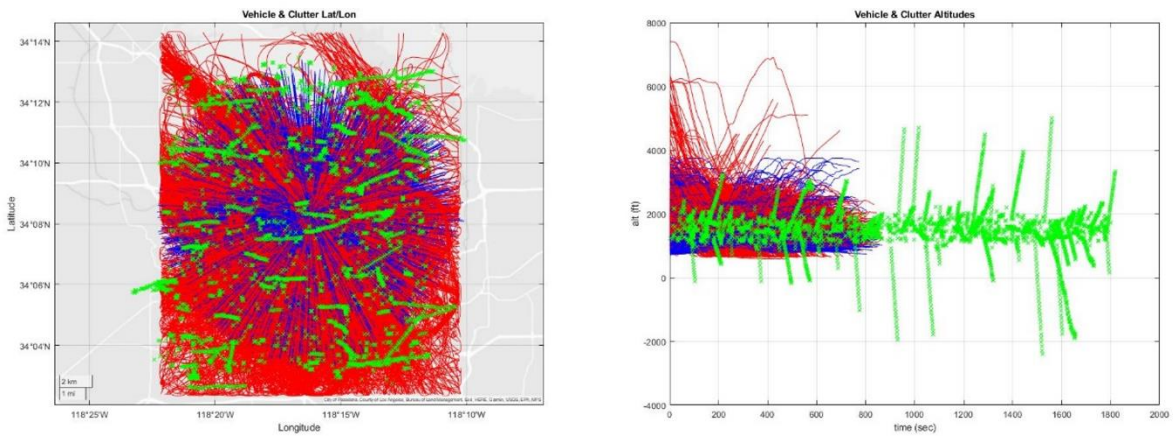


Figure 31. Medium density clutter.

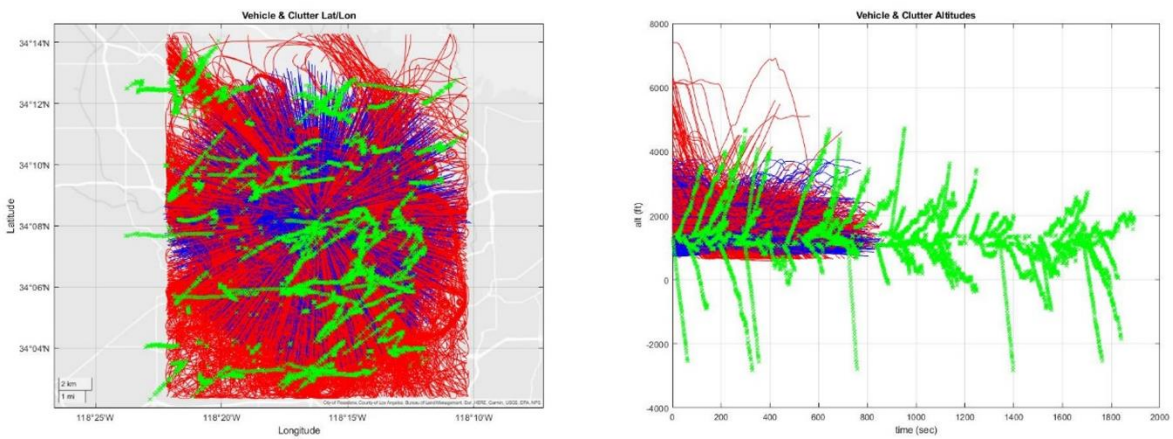


Figure 32. High density clutter. In these charts, ownship trajectories are shown in blue, intruders in red, and clutter in green.

Table 14 gives a summary of the safety statistics with each of the clutter datasets provided by MSU. Details for the clutter statistics can be found in Section 2.

Table 14. Summary of encounters using EO/IR sensor data with varying clutter characteristics. OpVal refers to previously published data from MIT for the same encounters, Results are from simulations conducted in this work, and the Target are the ASTM LoWC ratio and NMAC risk ratios. (Note, reduction in safety statistics are due to likely simulation bias as noted in 3.2.1)

Clutter Level	Alerting Encounters	LoWC (with DAA/no DAA)	NMAC (with DAA/no DAA)	RR (LoWC)	RR (NMAC)	P(LoWC)	P(NMAC)	SLoWC (mean)	SLoWC (>33%)
				OpVal					
				Results					
				Target					
None	9233	234/2716	1/213	0.0900	0.0045	0.0253	1.08e-4	8.62	0.00140
				0.0862	0.0047				
				0.4000	0.1800				
Low	9092	271/2716	1/213	0.0998	0.0047	0.0294	1.1e-4	9.50	0.0018
Medium	9193	273/2716	2/213	0.1005	0.0094	0.0296	2.2e-4	8.52	0.0017
High	9169	251/2716	2/213	0.0924	0.0094	<b>0.2720</b>	2.2e-4	9.460	0.0014

### 3.3.2 Operational Suitability Analysis

The operational suitability analysis was repeated using the model-based clutter data and showed a noticeable effect using the MSU clutter data. Figure 33 shows that the EO clutter led to a significant increase in alert duration and a noticeable increase in the number of split alerts. Neither clutter data set caused a significant increase in horizontal or vertical reversals.

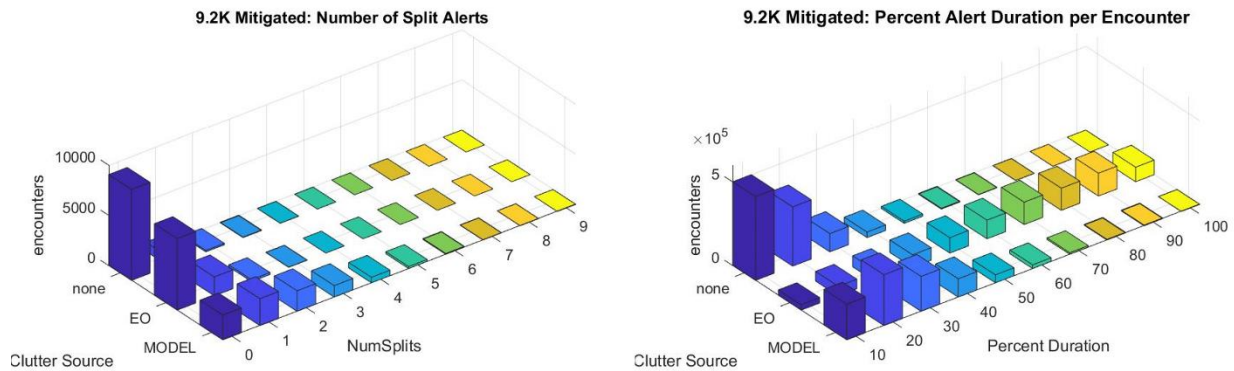


Figure 33. Number of split alerts and alert durations per encounter for model-based clutter.

### 3.3.3 MSU Clutter Data: Safety Analysis

The safety analysis performed on simulation results obtained using the MSU clutter data was similar to what was obtained using the OSU GBR clutter. The EO clutter caused a relatively small increase in LoWC while the model-based clutter caused a relatively small decrease in LoWC.

Table 15. Analysis using alerting encounters with model-based clutter data. (Note, reduction in safety statistics are due to likely simulation bias as noted in Section 3.2.1)

Clutter Level	Number of Alerts	LoWC (with DAA/no DAA)	NMAC (with DAA/no DAA)	RR (LoWC)	RR (NMAC)	P(LoWC)	P(NMAC)	SLOWC (mean)	SLOWC (>33%)
				OpVal					
				Results					
				Target					
None	9233	234/2716	1/213	0.0900	0.0045	0.0253	1.08e-4	8.62	0.00140
				0.0862	0.0047				
				0.4000	0.1800				
EO	9201	279/2716	2/213	0.1027	0.0094	0.0302	9.4e-3	9.18	0.00140
Synthetic EO/IR Data	9203	181/2716	2/213	0.0666	0.0094	0.0196	2.6e-4	8.97	0.00130

## 4 TERMINAL MODELING AND SIMULATION RESULTS

### 4.1 Simulation Setup

From the one million trajectories, 20,000 were selected for clutter testing in MSU’s modeling and simulation system. Down sampling was accomplished by defining an approach corridor corresponding to a full-scale deflection of the approach indicators used for precision Instrument Landing System (ILS) or Area Navigation (RNAV) approaches. Details for the geometry of this corridor are provided in Figure 34. During the simulated encounters, if the aircraft penetrated this boundary, the approach was terminated and tabulated as a missed approach. It should be noted that adopting the corridor width corresponding to a full deflection of the guidance cues provided during standard IFR operations is somewhat dubious. This wider corridor boundary used in simulation allowed for using more trajectories in the MIT dataset owing to the Bayesian framework they were generated with. The number of deviations resulting in the ownship aircraft departing the corridor boundary due to a DAA alert are expected to underrepresent the number of actual departures out of an actual ILS approach that had a more realistic corridor. However, the results presented in the following sections can still be interpreted in a way that makes the impact of clutter obvious in the trends surrounding missed approaches, LoWC, etc. even though impacts may be underrepresented. Figure 35 shows the resulting down sampled approaches in pink, superimposed on a larger subset of the trajectories in blue. The next section details the modeling and simulation results obtained using MSU’s simulation environment with these ownship and intruder models with varying levels of clutter provided by ground-based DAA sensors.

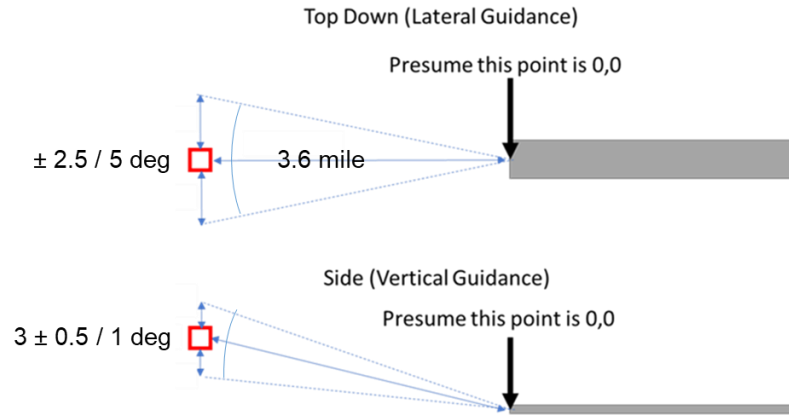


Figure 34. Approach corridor definition for lateral boundaries (top), and vertical boundaries (bottom).

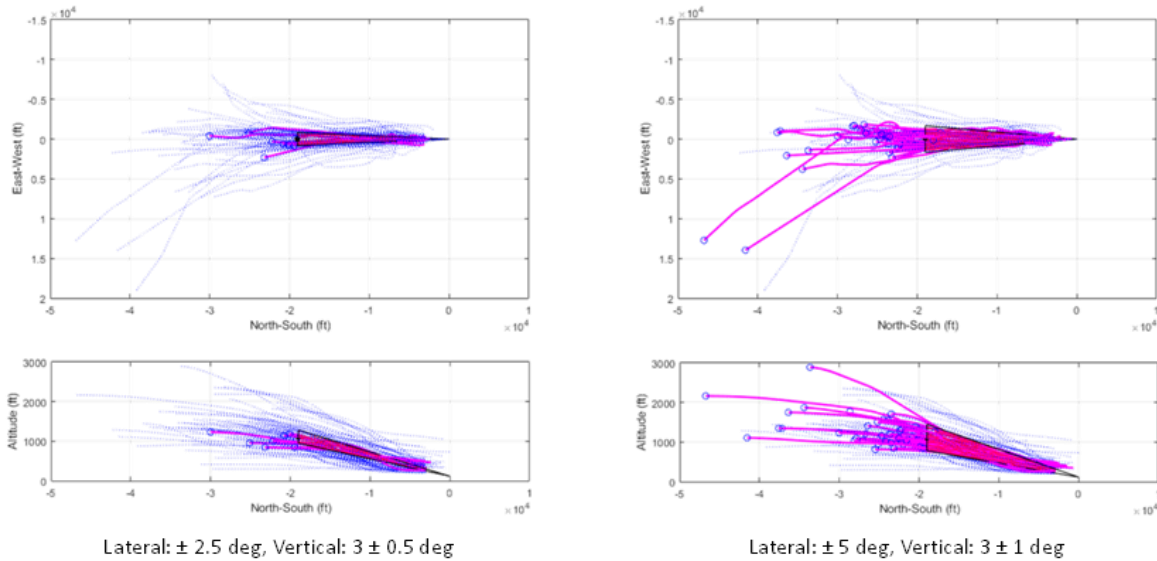


Figure 35. Subset of ownship trajectories meeting the missed approach threshold requirements, shown in pink. Blue tracks do not intersect the approach corridor and were discarded.

#### 4.2 Ground-Based EO/IR Results

Figure 36 to Figure 39 illustrate four levels of clutter data (Low, Medium, Medium High, and High) distributed within an approximate 10,000 ft radius from the origin, identified as the airport. In these figures, the clutter-flux density is similar to the previous enroute testing and summarized in Table 16. Each figure is organized from left to right, beginning with unfiltered raw data and followed by data processed through two types of filters. These two filtered views of the data are based on the assumption that clutter is significant if the radar has maintained tracking for at least three or five seconds, respectively. This approach allows for distinguishing meaningful clutter from transient data. Table 17 provides a summary of the total number of samples and tracks associated with each filter type and indicates the impact of filtering. The total number of samples in Table 17 represents the amount of data collected by the sensor over a 30-minute period, and the

number of tracks refers to the count of sequentially meaningful data points assigned arbitrary identifiers within the collected data. Notably, differences across clutter levels are observed, with an approximate variation of 600 samples and around 50 tracks per level, reflecting how filtering can reduce noise and improve the clarity of significant radar returns.

Table 16. Clutter-flux densities tested in the terminal environment in false tracks/(nm<sup>2</sup>-hr).

<b>Filter</b>	<b>High</b>	<b>Med-high</b>	<b>Med</b>	<b>Low</b>
<b>None</b>	437	315	188	85
<b>3s</b>	113	83	53	21
<b>5s</b>	68	52	31	13

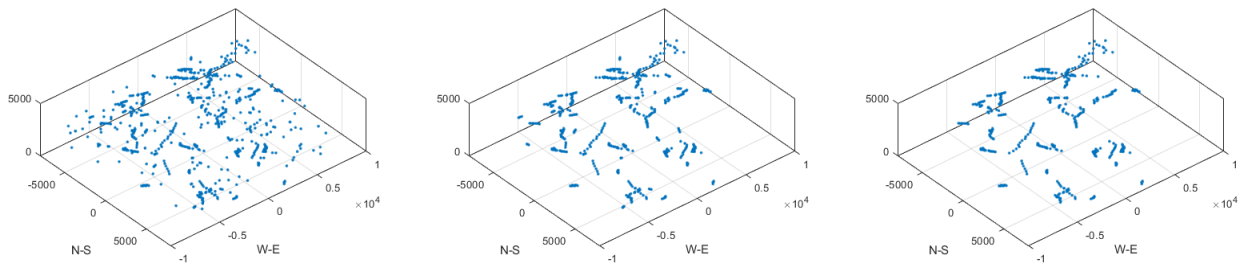


Figure 36. Low-rate clutter raw (left), with 3 second filter (middle) and 5 second filter (right).

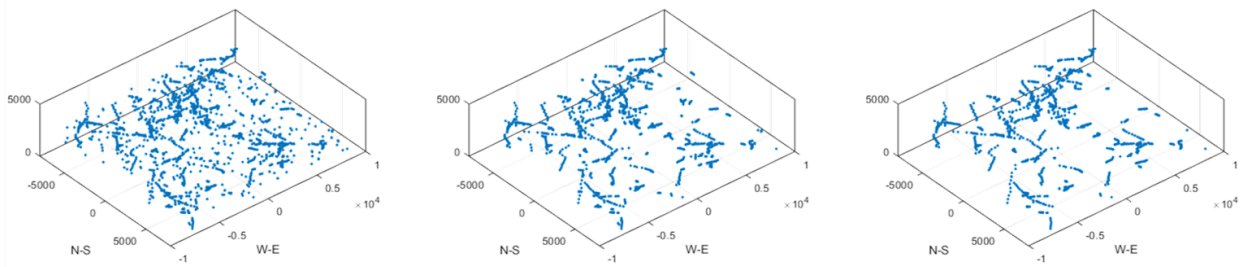


Figure 37. Medium-rate raw (left), with 3 second filter (middle) and 5 second filter (right).

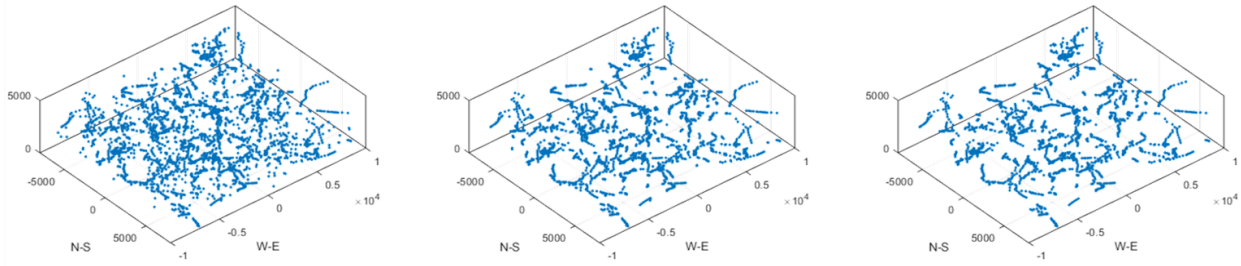


Figure 38. Medium-high rate raw (left), with 3 second filter (middle) and 5 second filter (right).

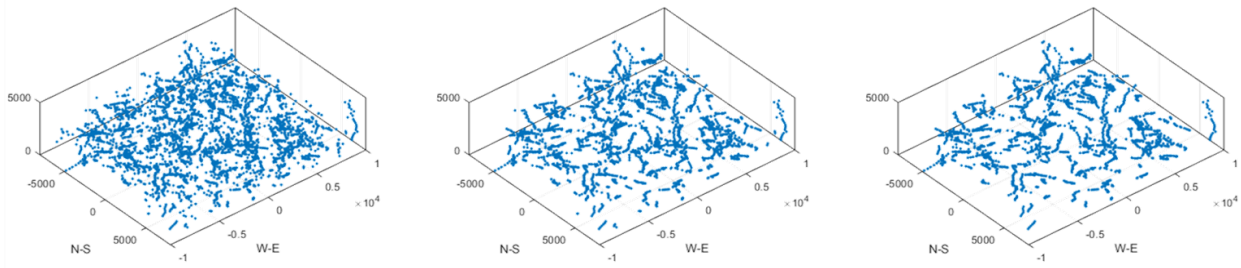


Figure 39. High-rate raw (left), with 3 second filter (middle) and 5 second filter (right).

Table 17. Number of samples and tracks for different levels of clutter on filtering options.

Clutter Levels	Filter	Number of samples	Number of tracks
Low	No filtering	862	256
	3s filtering	645	64
	5s filtering	566	41
Medium	No filtering	2013	564
	3s filtering	1546	160
	5s filtering	1310	93
Medium High	No flittering	3197	946
	3s filtering	2394	250
	5s filtering	2069	156
High	No flittering	4266	1311
	3s filtering	3125	340
	5s filtering	2652	204

This report conducts a detailed analysis of clutter's impact by examining four distinct cases that incorporate one intruder and varying levels of clutter across four configurations. Figure 40 provides a key to the symbols used in the graphs shown in Figures 41 through 45. In situations of Loss of SST or Loss of ART, the colors of the information related to the ownship change, and when clutter enters the ART, it is represented by red rectangles with an indication of the direction of movement, which is a notable feature. In a Loss of ART situation, the desired heading of the ownship points to the mid-angle of the recovery band. Figure 41 through Figure 44 depict the chronological progression of flight trajectories for each of these configurations: (1) ownship only, (2) ownship + intruder, (3) ownship + clutter, and (4) ownship + intruder + clutter. An example scenario featuring a certain encounter set with low-level clutter is provided for clarity in assessing the influence of variables and to enhance the reliability of the findings. In Figure 41, the flight adheres to a funnel-shaped landing approach typical of the ownship-only scenario, demonstrating a direct and stable approach path. [consider adding a description of the approach corridor represented by the gray wedge, a dotted track tail, a ghost path that the drone is attempting to follow for the ILS approach, and helping the reader to interpret what the forward projected black and blue lines are. Likewise consider helping the reader with descriptive text to know what the red lines are for the intruder, to notice how ownship lines change colors with alerts, etc. I had to study it for a while and still have a few questions]. Figure 42 through Figure 44 provide a more complex picture; in the second and third graphs of each, the timing and nature of evasive maneuvers executed to avoid the intruder or clutter are displayed, with the final graph showing the trajectory as the ownship approaches the target. Figure 45 expands this analysis to illustrate the final trajectories under varying levels of clutter for the most complex case: ownship + intruder + clutter. As clutter intensity increases, the frequency and complexity of evasive maneuvers intensify, resulting in highly intricate flight paths that significantly diverge from the standard approach, underscoring the substantial influence of clutter on flight path behavior as the ownship attempts to reach its target.

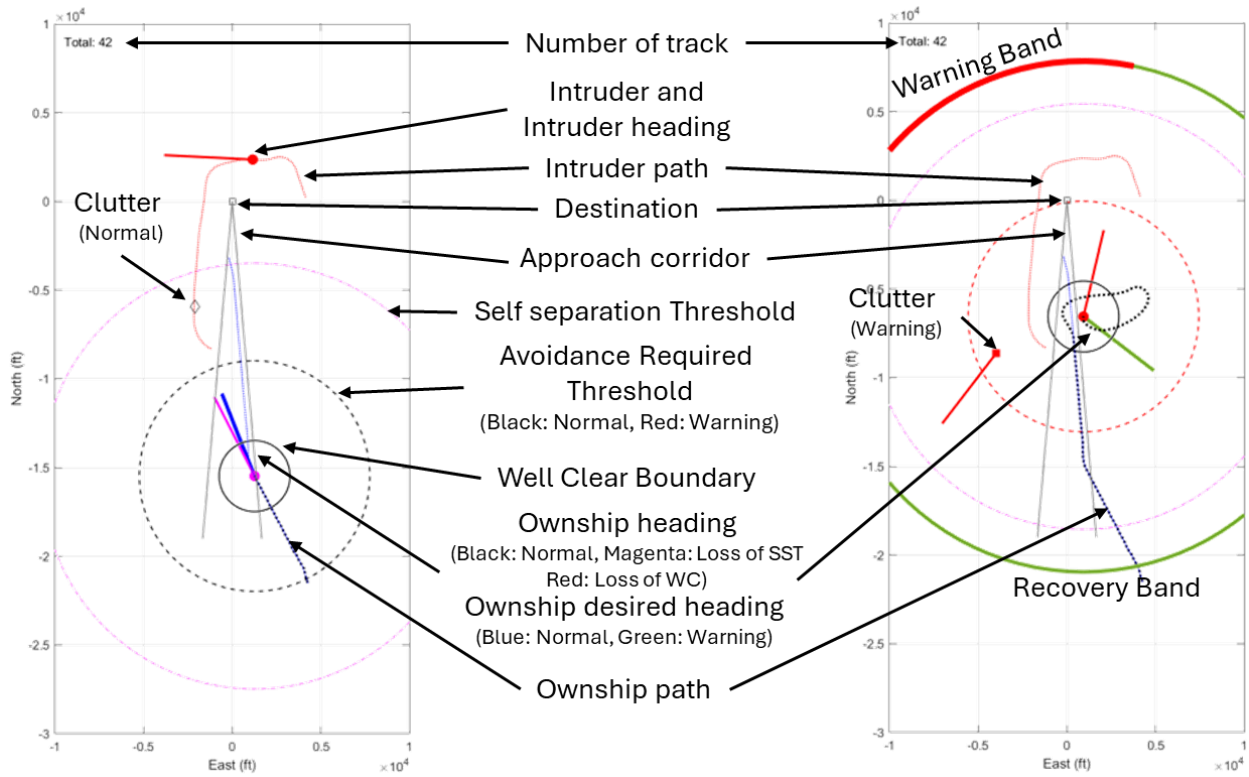


Figure 40. Description of symbols used in the trajectory graphs shown below.

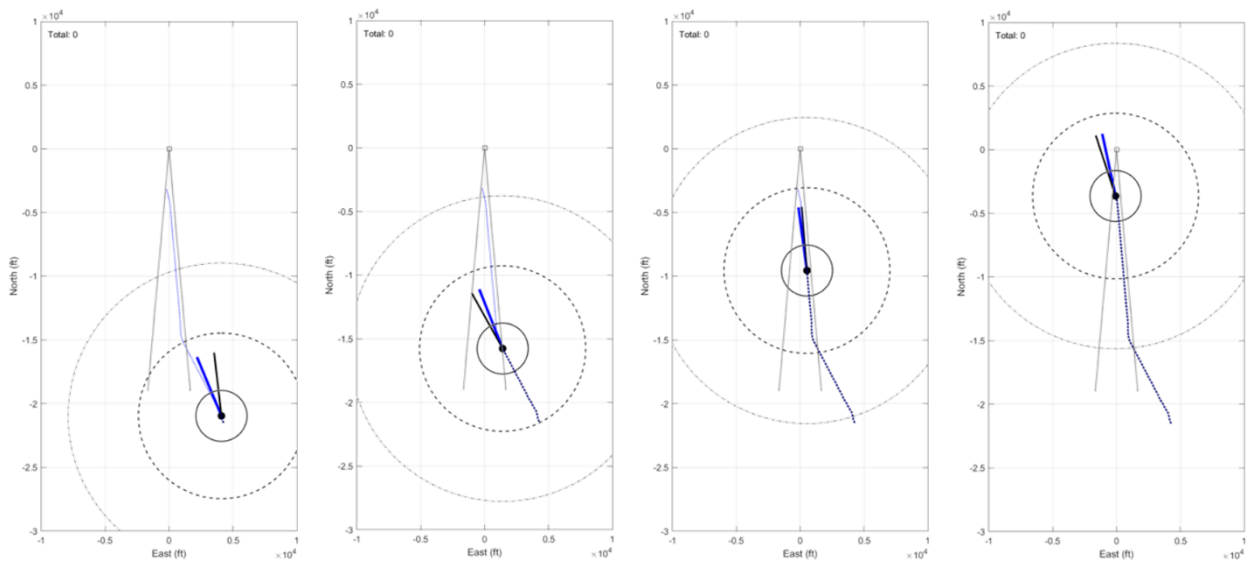


Figure 41. Flight trajectory in chronological order (left to right) of ownship-only case.

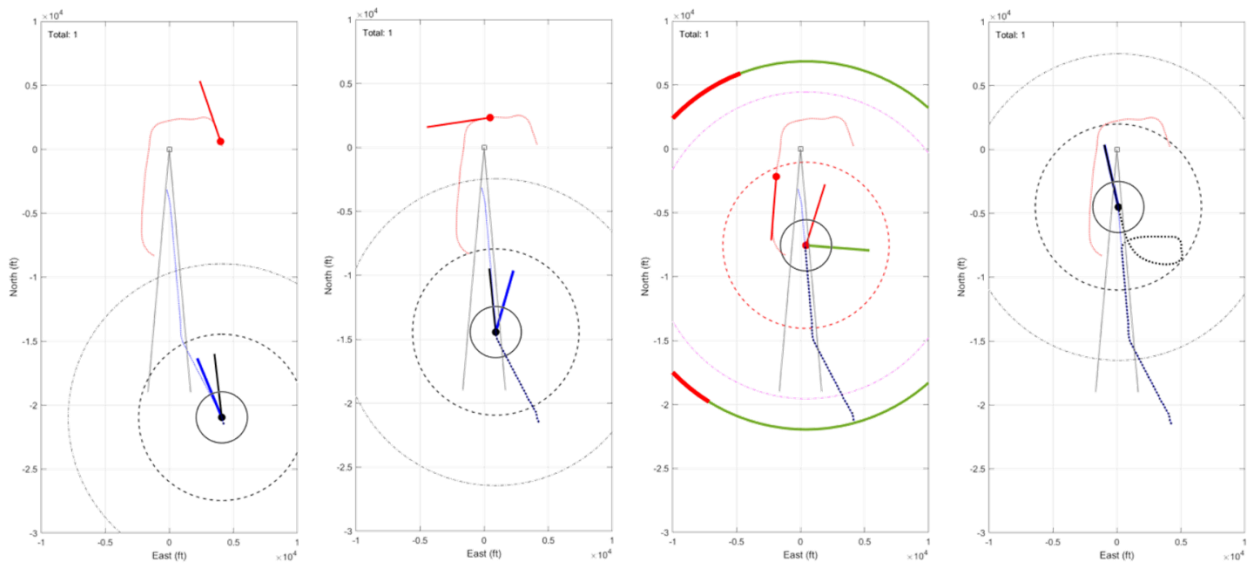


Figure 42. Flight trajectory in chronological order (left to right) of ownship + intruder case.

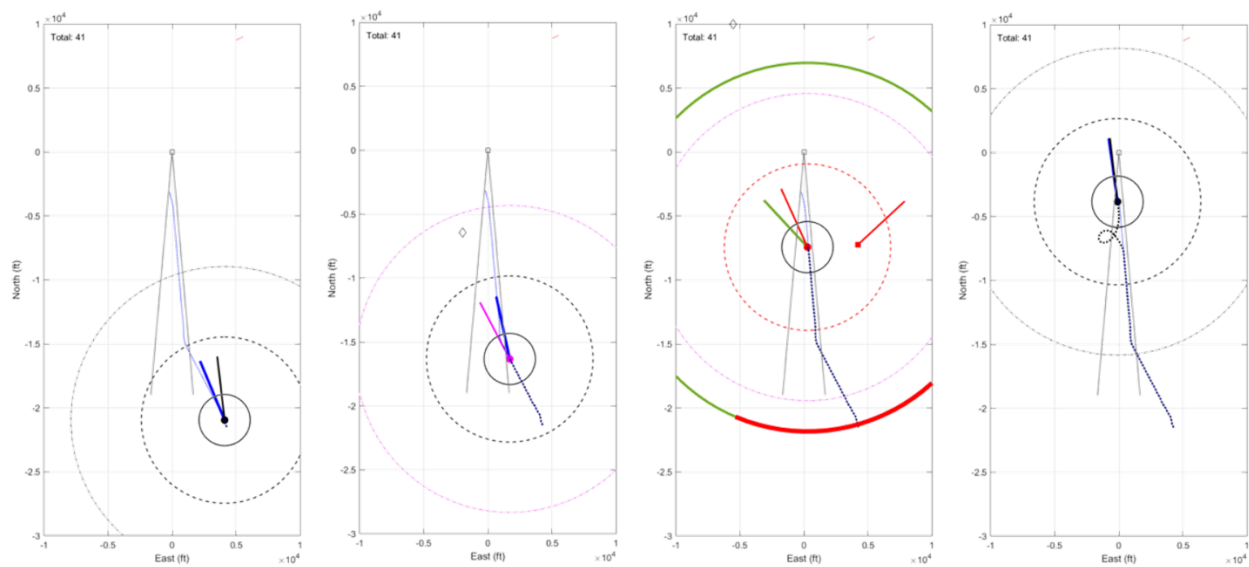


Figure 43. Flight trajectory in chronological order (left to right) of ownship + clutter (Low) case.

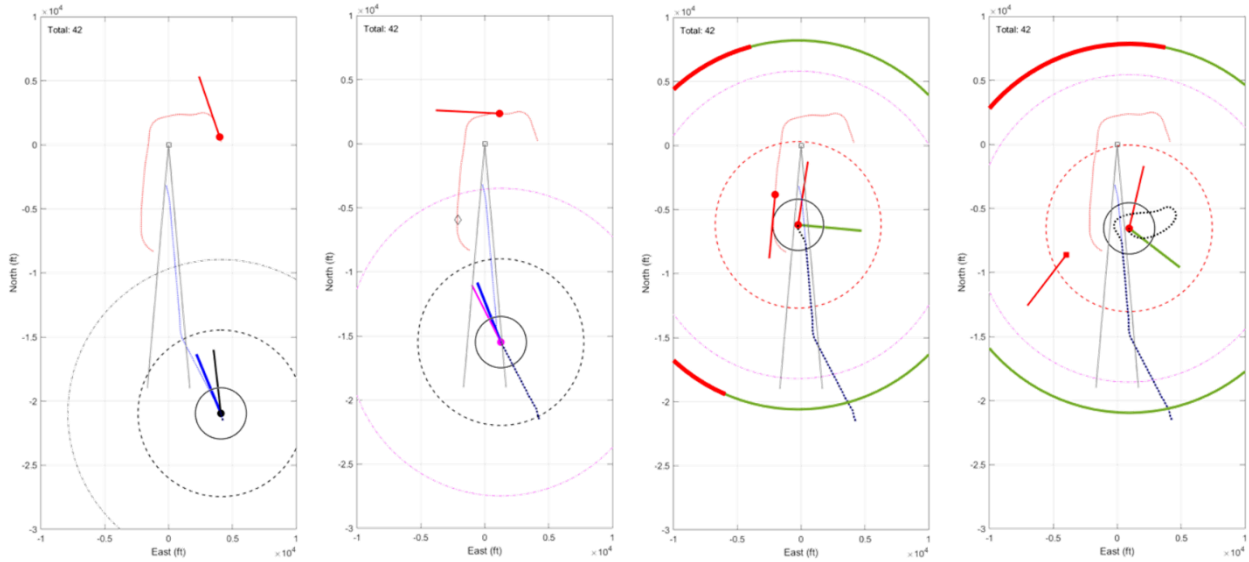


Figure 44. Flight trajectory in chronological order (left to right) of ownership + intruder + clutter (Low) case.

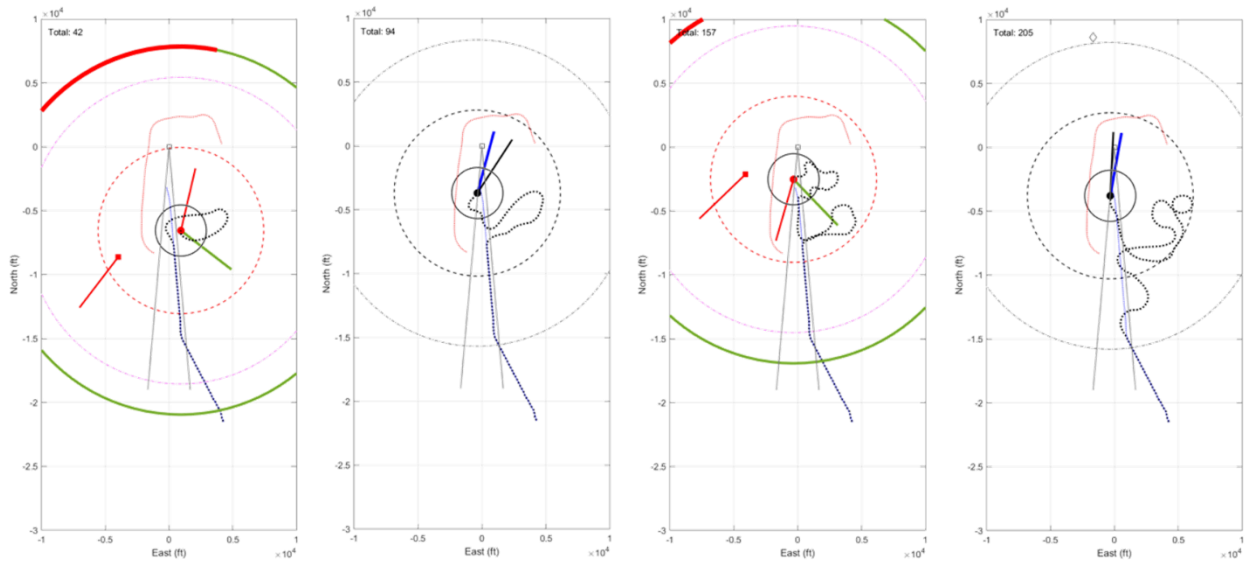


Figure 45. Flight trajectory of ownership + intruder + clutter for Low/Medium/Medium High/High (left to right) cases.

While the preceding figures give some qualitative indication of the impact of clutter density on an individual flight path, the quantitative statistics give a more complete picture. First, the impact of filtering is considered for four different scenarios, 1: Ownship only, 2: Ownship + intruder, 3: Ownship + clutter, and 4: Ownship + intruder + clutter. The data is presented in this way to allow the reader to provide a baseline when comparing increasingly complex operational scenarios and so the effect of the ownship maneuvering relative to the intruder versus clutter can be better understood. Tables 18 and 19 provide the statistics for the average alerts per flight and average alerts per minute for the four outlined cases using three- and five-second filters. The ownship-only

cases provide a benchmark of the simulation by producing no alerts, and the ownship + intruder data corresponds to the selection of 10k nominally alerting and 10k non-alerting cases (alerting roughly half the time). The ownship + clutter data gives a substantial rise in the number of alerts and the duration under alert, indicating a significant impact on operations, especially in the high-clutter case with 40 alerts and 15 minutes spent under alert. The final case considering ownship+intruder+clutter shows a general increase in the number and duration of the alerts, except in the high-clutter case. It is believed that the high-clutter case produced increasingly erratic guidance cues and reversals pushing the ownship further away from the intended landing path and the intruders, much like the results presented for the enroute operations. Therefore, this decrease in alerts should not be viewed as somehow beneficial. Table 19 considers the same cases with a five-second filter applied to the clutter data. Here, the benefits of increasing the filter time primarily affect the medium-high and high filter data, reducing the number and time under alert by half. However, for a nominally three- to four-minute approach, this still results in approximately one alarm every 7.5 seconds.

Table 18. Average of alerts per flight and average of alerts per minute for 3-second filtered clutter data.

3 sec filtering	low		medium		medium-high		high	
	Total	/ min	Total	/ min	Total	/ min	Total	/ min
<b>Ownship</b>	0.00	0.00	0.00	0.00	0.00	0.00	0.00	0.00
<b>Own + Int</b>	0.52	0.24	0.52	0.24	0.52	0.24	0.52	0.24
<b>Own + Clu</b>	0.23	0.11	7.21	4.11	16.46	5.25	39.36	14.51
<b>Own + Int + Clu</b>	1.39	0.61	6.85	3.14	20.54	6.43	35.82	12.68

Table 19. Average of alerts per flight and average of alerts per minute for 5-second filtered clutter data.

5 sec filtering	low		medium		medium-high		high	
	Total	/ min	Total	/ min	Total	/ min	Total	/ min
<b>Ownship</b>	0.00	0.00	0.00	0.00	0.00	0.00	0.00	0.00
<b>Own + Int</b>	0.52	0.24	0.52	0.24	0.52	0.24	0.52	0.24
<b>Own + Clu</b>	0.21	0.10	6.81	2.41	8.26	3.97	21.10	7.96
<b>Own + Int + Clu</b>	1.35	0.60	6.18	2.90	12.23	3.48	16.01	5.85

Note that in Table 19 even under low clutter conditions with 5 seconds of filtering, that the Ownship + Clutter case results in 0.21 alerts per approach flight. In other words, in roughly 20% of simulated approaches the low clutter case resulted in the ownship receiving a DAA alert and maneuvering to avoid a perceived intruder that was actually a clutter track. This amount of ownship avoidance maneuvering would likely have a significant impact on ATC coordination and ATC

communication with the remote pilot as compared to existing operations today where very few crewed aircraft perform an avoidance maneuver while on approach because ATC has already separated them from most of the traffic. The results of the low clutter case with a 20% likelihood of a DAA alert on approach suggests that even more robust track classification and filtering are needed for good integration of UAS into airport environments than the low clutter case. The medium (6.81), medium-high (8.26), and high clutter (21.1) cases are worse with multiple DAA alerts and maneuver actions occurring due to clutter for every approach attempt.

Tables 20 through 23 detail the impacts of increasing clutter levels on missed approaches, LoWC, NMACs, and reversals. In this data, the baseline cases selected resulted in 6.5% of approaches being missed. This is higher than real-world estimates of IFR operations in instrument meteorological conditions (Blajev & Williams 2017) and is a result of the Bayesian path generation in the MIT dataset. Using this higher missed approach baseline, the effects of clutter are still clearly evident, with a nearly 6-fold increase in the high-clutter case. It should be noted that the final case of ownship+intruder+clutter is not additive owing to the maneuvering taking place. The statistics for LoWC and NMACs generally follow the same trends, with a substantial increase in both for the high-clutter case. Reversals also increase with clutter levels to nearly 100% in the high-clutter case, equating to a severe impact on airspace usability.

Table 20. Missed approach percentage, LoWC, NMAC, and reversals for low-clutter case (5s filter).

<b>Low clutter 5 second filtering</b>	<b>Missed Approach</b>	<b>LoWC</b>	<b>NMAC</b>	<b>Reversals</b>
<b>Ownship only</b>	6.5%	0.0%	0.0%	0.0%
<b>Ownship + Intruder</b>	27.5%	2.6%	0.0%	0.0%
<b>Ownship + Clutter</b>	12.3%	1.0%	0.0%	0.2%
<b>Ownship + Intruder + Clutter</b>	31.4%	6.4%	0.6%	44.1%

Note that Ownship + Clutter results in 5.8% more missed approaches than Ownship only. Even in low clutter, the increase in missed approaches due to clutter may be significantly more than the existing rate of real-world IFR missed approaches. When combined with the simulation setup that underrepresents missed approaches due to the use of a wider simulation approach corridor, the results suggest that even low clutter conditions may not be adequate for good UAS integration when on approach.

Table 21. Missed approach percentage, LoWC, NMAC, and reversals for Med-clutter case (5s filter).

<b>Medium clutter 5 s filtering</b>	<b>Missed Approach</b>	<b>LoWC</b>	<b>NMAC</b>	<b>Reversals</b>
<b>Ownship only</b>	6.5%	0.0%	0.0%	0.0%
<b>Ownship + Intruder</b>	27.5%	2.6%	0.0%	0.0%
<b>Ownship + Clutter</b>	17.0%	24.1%	1.2%	16.7%
<b>Ownship + Intruder + Clutter</b>	36.3%	27.7%	2.3%	56.5%

Table 22. Missed approach percentage, LoWC, NMAC, and reversals for Med-High-clutter case (5s filter).

<b>Med-High clutter 5 s filtering</b>	<b>Missed Approach</b>	<b>LoWC</b>	<b>NMAC</b>	<b>Reversals</b>
<b>Ownship only</b>	6.5%	0.0%	0.0%	0.0%
<b>Ownship + Intruder</b>	27.5%	2.6%	0.0%	0.0%
<b>Ownship + Clutter</b>	38.5%	29.4%	4.3%	61.8%
<b>Ownship + Intruder + Clutter</b>	67.6%	43.9%	6.8%	75.1%

Table 23. Missed approach percentage, LoWC, NMAC, and reversals for High-clutter case (5s filter).

<b>High clutter 5 s filtering</b>	<b>Missed Approach</b>	<b>LoWC</b>	<b>NMAC</b>	<b>Reversals</b>
<b>Ownship only</b>	6.5%	0.0%	0.0%	0.0%
<b>Ownship + Intruder</b>	27.5%	2.6%	0.0%	0.0%
<b>Ownship + Clutter</b>	68.1%	63.8%	6.4%	91.3%
<b>Ownship + Intruder + Clutter</b>	78.9%	48.5%	5.1%	82.4%

## 5 CLUTTER IMPACT ON OPERATIONS

### 5.1 Overview

MSU conducted a series of live flight DAA tests using a large UAS and a crewed aircraft in various encounter geometries. The large UAS was equipped with a multi-camera DAA system capable of detecting intruder aircraft at distances of several thousand feet. Additionally, a cooperative ADS-B In sensor captured signals from nearby aircraft, including the crewed test aircraft.

Encounters were designed to produce horizontal NMACs with a variable safety offset in the vertical direction for safe flight testing. Live aircraft detection data was streamed to a dedicated User Interface in the Ground Control Station (GCS), displaying the relative position of any detections for UAS pilots.

These tests provided researchers with field data on true and false detections for future simulation modeling. Upon completion of the flight test program, pilots and flight test engineers were surveyed for qualitative feedback on the overall user experience, troubleshooting issues, and the effect of clutter on maintaining well clear of the crewed aircraft.

## 5.2 Description of Systems

To mitigate potential system faults and the risk of DAA system crashes or corruption of the primary autopilot's software, researchers integrated an isolated secondary autopilot with telemetry sensors. This autopilot communicated with the onboard GPS, non-cooperative and cooperative sensors, and relayed data to a companion computer responsible for downlinking information to the GCS.

The system architecture included:

1. A primary autopilot for core flight functions;
2. An isolated secondary autopilot for DAA operations;
3. Cooperative (ADS-B) and non-cooperative sensors;
4. A companion computer for data processing and downlink; and
5. GCS visualization software for pilot interface.

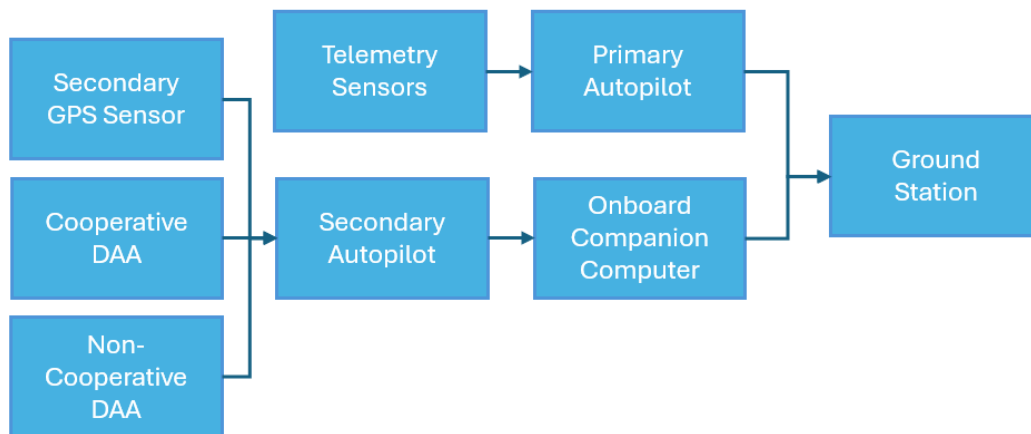


Figure 46. Basic schematic of the primary and the isolated secondary autopilot onboard the large UAS.

The GCS software displayed cooperative and non-cooperative detections differently, with pilots trained to distinguish between them. The system generated alerts of varying severity, visualized as yellow or red arcs on the user interface, indicating threat locations and areas where the ownship aircraft should avoid maneuvering. Aural alerts using the term "traffic" complemented the visual indicators.

## 5.3 Field Tests

Researchers developed test plans to evaluate the interaction between a large UAS and various crewed aircraft at different altitude separations, assessing the DAA system's effectiveness. Secondary objectives included gathering qualitative data on the visualization software's ability to

logically position intruders relative to the ownship, and the impact of visual and audio alerts on pilot awareness.

A "wagon-wheel" approach was employed to vary relative angles between the ownship and intruder. Over 100 encounters were conducted using these configurations:

- 1) Non-cooperative sensor and cooperative sensor on and alerting;
- 2) Only non-cooperative sensor on and alerting; and
- 3) Only cooperative sensor on and alerting.

For each encounter, the crewed aircraft varied its flight plan to achieve the desired geometry, while the UAS maintained a predefined North-South repeating path under GCS pilot supervision. Safety margins were maintained through established "Knock-it-off" criteria.

#### **5.4 Surveys**

A short list of research questions was targeted for the field testing of the system of systems within the flight test plan. Researchers wished to understand the role of the visualization and alerting system in the GCS cockpit, and to what level the systems benefit or increase the workload for the pilots. The following lists the basic questions researchers sought responses for.

- A. How might the additional display (the DAA user interface within the GCS) have added workload to your PIC duties?
- B. What possible situational awareness benefits did you encounter from the additional sensors?
- C. Were there any issues or troubleshooting with the additional hardware and software?
- D. How often were you distracted by unnecessary alerts or information being displayed?
- E. What do you believe caused this distraction?

The research team, including the pilots and flight test engineers, individually answered and were given time for any additional unprompted comments.

#### **5.5 Results**

Only two of the previously planned configurations were tested, as the growing understanding of the system and its limitations prompted the cancellation of the third (cooperative sensor only) configuration.

One key finding was the onboard non-cooperative sensor detected the intruding aircraft during every encounter, and on its own, in the second configuration, rarely detected clutter nor alerted falsely.

Therefore, the results focus on the first configuration in which either sensor could detect clutter, other non-test aircraft, or contribute in some way to the alerting pipeline. Figure 46 visualizes a world cloud of the common responses from the field testing for prompt E regarding the possible sources of the distractions generated by the GCS visualization tool. Extraneous or irrelevant words were thrown out to parse the data for analysis.

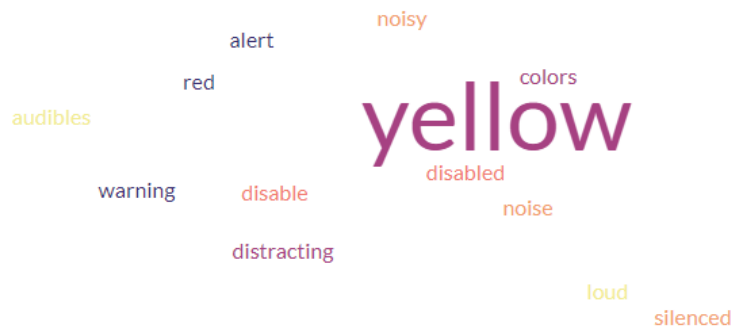


Figure 47. Word cloud of most prominent words, visualized by larger fonts, used by the research team when qualitatively evaluating the DAA system's clutter.

The most repeated word was found to be “yellow,” as the team found in testing that the “alerting band” the DAA algorithm used to visualize intruders that may become a threat most often appeared on the user display. This yellow band would generally also be accompanied by an audio cue to alert the operators of an intruder track being processed by the DAA algorithm. Important to note is the test area was limited to near airport operations due to Visual-Line-of-Sight restrictions. However, both test aircraft were vertically displaced from the airport operational volume. Throughout the tests, a few general aviation aircraft either entered the terminal airspace, taxied, or took off from the runway. The results showed that in many instances, aircraft that the large UAS operators would normally not concern themselves with tracking during nominal operations would cause these yellow-banded alerts. In post-processing of the data, it was determined that grounded air traffic that were broadcasting ADS-B were the source of the alerts.

Several responses included words such as noisy, noise, or sound-related terminology, indicating that the research team felt the audible alerts were distracting during the tests. In cockpit audio recordings, researchers determined several instances where a single intruder produced multiple audible alerts to the pilots.

After collecting data on several encounters between the two aircraft participating in the tests, and in response to the presence of the nuisance alerts, the flight test team elected to turn off the alerting algorithm and continue testing with only visualization of ADS-B and non-cooperative tracks enabled. This led to the conclusion that the system of systems being evaluated should likely not operate with alerting enabled while performing terminal airspace operations, and alternative strategic or technical mitigations should be put in place to maintain an acceptable level of safety.

## 5.6 Recommendations

The research team recognizes the challenges of the systems used and the environment in which the systems were tested. The team determined a short list of recommendations for the system to be more operationally suitable.

The first recommendation relates to the number of alerts per intruding aircraft. As the presence of an intruder in nominal operations is generally an infrequent occurrence, pilots already compartmentalize a portion of their workload dedicated to tracking that intruder. Repeated audible alerts should be minimized.

Second, a positive addition for user experience for any DAA display may be the ability to select and “cancel” certain tracks that the pilots can logically rule out. As traffic well outside of the test area but of known intention (such as a student and instructor pilot practicing touch and go’s) repeatedly became a visual and aural nuisance, the two member team of pilots operating the large UAS suggested an ability to select or drag the cursor over the interface to remove the traffic from the alerting cycle.

Last, as every alerting arc or band was similar in width, in some instances the full 360-degrees around the aircraft became a yellow alerting band. This was caused by the presence of multiple intruders. Given no maneuver guidance, for this system, is ever provided for yellow alerting-level events, adding variable width of the arcs based on the proximity to the intruder causing that alert could help pilots quickly figure out which aircraft alert may soon evolve into higher severity alert levels.

## 6 CONCLUSIONS

This report outlines three different definitions for clutter used in the airspace analysis presented in Section 1. Namely, the first represents a pseudo flux of false tracks, normalized by a unit area ( $\text{nm}^2$ ) per unit time (hr). This flux appears throughout the remainder of the document and is the primary metric considered in the safety analyses as it represents both the spatial and temporal aspects of the clutter field and is easily scalable between encounter sets. When working with data collected from different DAA sensors, it becomes clear that clutter is not uniformly distributed in space or time. In this case, it may depend to first order on the sensitivity of the sensor to various environmental inputs such as birds, trees, reflections, moving ground targets, etc. In this case, it is instructive to consider the clustering of the clutter elements, or put more simply, the relative density of clutter at any given time. This metric captures what is often encountered in ground-based sensors such as radar and EO/IR systems. Finally, a hybrid of the two is presented as a navigable fraction, or the likelihood of encountering clutter relative to the total amount appearing at any one time (related to clustering but considers ownship dynamics and DAA specifications).

These metrics are used in conjunction with the encounter sets extracted from the MIT TCAS/MITRE dataset used in characterizing sXu for enroute encounters. This dataset was a suitable candidate for evaluating the effect of CFD as the range of vehicle speeds and altitudes were commensurate with the operating environments considered in this work. For fast-time simulations, a broad encounter set was chosen to allow for the incorporation of different clutter densities. This encounter set includes one million individual encounters corresponding to terminal to up-and-away flight trajectories. A second set of tests were conducted using terminal encounters extracted from datasets provided by MIT Lincoln Labs for straight-in approaches into a Class D airport with a single intruder. From this dataset, 20,000 trajectories were selected which corresponded to a standard approach boundary provided by an onboard course deviation and glideslope indicator. For the terminal encounters, the DAIDALUS DAA algorithm was used in lieu of sXu.

The encounter geometries provided the test cases for assessing the impact of various clutter fluxes and spatial/temporal characteristics. For this work, real data provided by ground-based radar systems and EO/IR sensors was chosen as it allowed for rapid tuning and evaluation of the impact of fast-time clutter, or targets that appear randomly and persist for times on the order of seconds,

and clutter produced by birds/ground traffic that is highly correlated and persists for longer periods of time. Within these two domains, the clutter density could be varied by adding/removing entire tracks, thus modulating the CFD used within individual encounters. The ground-based radar had a nominal CFD of 260 false targets/(nm<sup>2</sup>-hr). This corresponds to approximately four false targets per square nautical mile per minute. I.E., in any one square nautical mile, there is a 95% chance that four false targets will appear every minute. Each of these tracks persists for approximately 16 seconds, corresponding to the tracking time constant built into the radar. While this certainly represents a substantial quantity of false tracks, it serves as a useful limiting test case in the safety evaluations. The Cassia-G model developed for the terminal environment produced a comparable level of CFD compared to the ground-based radar at OSU. This sensor was used to create a synthetic dataset outlined in Section 2 to allow for tuning of the clutter statistics. For the terminal encounters, a higher CFD of close to 437 false targets (nm<sup>2</sup>-hr) was used as the upper bound, corresponding to higher clutter densities expected to occur at altitudes below 1,000 ft above ground level.

### **6.1 Enroute Encounters**

For the enroute testing, the effect of CFD was evaluated by subdividing the 260 false targets/(nm<sup>2</sup>-hr) produced by the ground radar by powers of two with a lower bound of 47 targets/(nm<sup>2</sup>-hr) (>1 target/(nm<sup>2</sup>-min)). With the range of speeds considered in the enroute encounter sets, the ownship, flying at 30 kts, may encounter one to two false tracks per minute within one nautical mile. From the data presented in Section 3, the impact of this level of clutter with the maneuver bounds prescribed with sXu does not substantially change the LoWC or NMAC statistics compared to the baseline no-clutter case. As the CFD is increased, the total number of alerts also increases. It should be noted that the number of alerts is highly dependent on the simulation conditions, the most notable of which is the total simulation time. For the analyses presented in this report, the total simulation time is on the order of six minutes of flight time, corresponding to a UAS flying three nm at 30 knots. However, the trend of increasing alerts with clutter density does subsist when the total simulation time is changed. As a brief aside, the highest CFD from the ground-based radar is 260 false tracks/nm<sup>2</sup>-hr, equating to approximately four false tracks per nm<sup>2</sup>-min. To explore this effect in greater detail, the simulations were rerun with different initial conditions on the clutter (clutter tracks were moved in space and time). The resulting statistics are representative of the mean with low overall standard deviations in the LoWC, inferring some degree of invariance with the precise location or emergence time of any given clutter track.

Since the initial encounter set was highly saturated with alerting encounters, by definition, the ownship would be moving toward the intruder. Therefore, any deviation is likely to result in a short alert against the clutter and greatly reduces the chance that an alert will occur against the intruder (encounter bias) since no effort was made to return to the initial course. While an interesting observation, the real-world implications of random maneuvers while avoiding false clutter tracks likely create a far greater threat than any safety improvement offered by randomly maneuvering away from an encounter. This effect is likely multiplied in dense airspaces with multiple intruder aircraft, where any random path deviations may increase the likelihood of having an encounter with other intruder vehicles. However, it is academically interesting to note that the design of the simulations using existing encounter geometries with the inclusion of clutter is certainly not additive, owing to higher order effects such as random walk leading to the false notion that clutter improves safety.

Further tests on encounter sets including nominally non-alerting scenarios were also considered. This was done in an attempt to minimize the random walk effect noted earlier. In this case, 65,000 non-alerting cases were used in lieu of the alerting cases previously discussed. The resulting simulations resulted in an increase in LoWC with increasing clutter levels. This indicates that the effect of clutter “steering” the ownship away from an intruder (i.e. encounter bias) is to some degree geometry dependent and may have a supplemental effect of steering it away from one target and toward another.

In an attempt to address the time and random walk aspects of the encounter sets, a time offset was proposed in which the clutter was suppressed until the alert between the intruder and ownship was triggered. This prevented the ownship from moving away from the intruder ahead of the encounter and introducing an artificial bias in the simulations, a key source of variability in the LoWC and NMAC statistics presented. The results of this testing indicate that, there is still an increasing trend or alerts and reduced separation events with higher clutter levels. Future work should investigate more advanced flight models which incorporate a return to path function to assess a more realistic flight scenario. When the initial conditions were changed either via adding non-alerting trajectories or by adjusting the alerting time window, the random path fluctuations induced by clutter increased the total number of alerts and LoWC events. Moreover, the number of alerts and LoWC events scaled with the CFD.

Increasing the total number of alerts has a direct impact on the operational suitability of the system. The analysis presented in Section 3.2.6 indicated that increased clutter leads to a longer time spent in an alert state, but that time is split over multiple *separate* alerts. This would certainly lead to an increased workload and a potential impact on safety if the pilot began heuristically filtering the nuisance alerts. Of note, while the alert levels increased, maneuvers resulting in a reversal or splits were still infrequent, even with the highest level of clutter. This indicates that there is a low chance that multiple clutter tracks on approach will create conditions resulting in a reversal or split. While there are certainly many underlying factors to this, it is suspected that the short duration of the false tracks was the primary reason for the lack of increased reversals/splits.

The EO/IR data contained false tracks which were generally of longer duration (misidentified birds, etc.), but less frequent than the ground-based radar data. This difference is reflected in the small changes in alerts and LoWC, for the varying clutter levels. However, there was a substantial impact noted in the operational suitability analysis where a longer amount of time was spent in the alert state and the overall number of split alerts increased. Of note, the EO model detailed in Section 2.4 resulted in approximately the same number of alerts, but fewer LoWC events compared to the real sensor data. However, the reasons are likely due to variability in the initial conditions.

## **6.2 Terminal Encounters**

Terminal encounter testing used 20,000 down sampled trajectories derived from a dataset of one million, focusing on clutter's impact during precision approaches. Simulations evaluated four scenarios: ownship only, ownship with an intruder, ownship with clutter, and ownship with both an intruder and clutter. Clutter levels ranged from low to high, with data filtered to distinguish significant clutter from transient noise using three-second and five-second tracking thresholds.

Key findings revealed that clutter significantly disrupted flight path stability, especially under high clutter conditions. As clutter increased, evasive maneuvers became more frequent and complex, leading to deviations from standard approach paths. Metrics such as missed approaches, LoWC,

and NMACs showed substantial increases with clutter intensity. High-clutter scenarios led to nearly sixfold rises in missed approaches compared to baseline, (ownship-only) alongside increases in LoWC incidents and NMACs. Alerts per flight also rose sharply, with high-clutter scenarios generating alerts approximately every 7.5 seconds, even after filtering.

Filtering reduced clutter-related alerts but did not fully mitigate operational challenges, particularly in high-clutter cases where guidance cues became erratic, causing significant deviations from the approach path. The study also highlighted that clutter might significantly increase remote pilot in command workload and reduce airspace usability. Substantial increases in the number of missed approaches have a severe impact on airspace usability in the terminal environment and would likely result in an increased burden on ATC facilities. Current best estimates indicate that only 0.1-0.3% of instrument approaches result in a missed approach. In the lowest clutter case considered, the missed approach percentage was more than an order of magnitude higher than that when considering only the effects of clutter, highlighting the sensitivity of terminal operations to even very low clutter densities.

### **6.3 Clutter Impact on Operations**

MSU conducted DAA tests using a large UAS and crewed aircraft to evaluate the performance of cooperative and non-cooperative sensors in various encounter geometries. The system integrated a secondary autopilot, multiple sensors, and a GCS interface that displayed alerts as visual bands and aural cues. Tests revealed that non-cooperative sensors reliably detected intruders with minimal false alerts due to being operated well above potential sources of ground clutter, while cooperative sensors frequently produced nuisance alerts due to grounded aircraft broadcasting ADS-B signals. Repetitive audio alerts and visual distractions, such as persistent yellow alert bands, significantly increased pilot workload. Based on findings, researchers recommended minimizing redundant alerts, enabling pilots to cancel irrelevant tracks, and using variable-width alert bands to better indicate imminent threats. These improvements aim to enhance usability and safety, particularly in terminal airspace operations.

### **6.4 Future Research Needs**

Future research should focus on demonstrating the impact of clutter classification and filtering techniques on the scenarios and baseline data presented in this report. Simple techniques such as 3 & 5 second persistence filters used in the terminal encounters had a significant impact on the resulting number of alerts, alert duration, LoWC, and NMAC statistics. The impact of increasing the detection-to-track time was not considered in this work and would likely pose challenges in operating in maneuver-constrained environments such as the approach corridor presented herein. For ground-based radars used in this work, short duration tracks are highly correlated with atmospheric conditions (precipitation, etc.) and wildlife activity. Both of these sources have unique RCS characteristics which make them amenable to classification and filtering (Emshoff et al. 2021) without imposing a strict time limit on track initiation. Other techniques such as machine learning and artificial intelligence have shown immense promise in classification and filtering, but do not provide guarantees on probability of false positives (aircraft classified as bird for example). Investigation of these techniques applied to the terminal environment in particular could provide a substantial improvement in the CFD appearing at low altitudes. Recent work on reducing alerting

thresholds in the takeoff/landing phases of flight could be incorporated to assess the impact of reduced alerts on pilot acceptance (Hoffler et al. 2019).

Finally more work is needed on developing metrics to assess the nuisance value of clutter. In this work, alert rates, reversals, splits, and alert durations were used to assess non-safety related impacts of clutter. However, there was a larger impact of reducing confidence in the DAA systems that manifested from all of these sources, and likely others not captured in this work. The reduction in confidence led to the systems being deactivated in the terminal environment by the RPICs, which highlights the importance of assessing the human factors implications imposed by increased clutter.

## 7 REFERENCES

1. MIT Lincoln Laboratories, Unmanned Aircraft Terminal Area Encounters, accessed 2/2024, <https://www.ll.mit.edu/r-d/datasets/unmanned-aircraft-terminal-area-encounters>
2. FAA Air Traffic Organization, "Safety Management System Manual: April 2019", 121 pp., 2019.
3. Fu, D., Liao, G., & Xu, J. (2021). Clutter Subspace Characteristics-Aided Space-Time Adaptive Outlier Sample Selection Method. *Sensors*, 21(9), 3108. <https://doi.org/10.3390/s21093108>
4. Granström, K., Baum, M., & Reuter, S., "Extended Object Tracking: Introduction, Overview and Applications", Feb 2021.
5. Park, S. H., Chong, S. Y., Kim, H. J., & Song, T. L., "Adaptive Estimation of Spatial Clutter Measurement Density Using Clutter Measurement Probability for Enhanced Multi-Target Tracking. *Sensors*", 20(1), 114, 2020. <https://doi.org/10.3390/s20010114>
6. U.S. Department of Transportation, "Safety Risk Management Policy", FAA Order 8040.4C, pp. 40, 2023a.
7. U.S. Department of Transportation, "Unmanned Aircraft Systems Safety Risk Management Policy", FAA Order 8040.6A, pp. 30, 2023a.
8. Blajev, Tzvetomir; Curtis, William, "Go-Around Decision-Making and Execution Project", Flight Safety Foundation. March 2017.
9. Bijjahalli, S., Gardi, A., & Sabatini, R. (2021). A novel detect-and-avoid approach for UAS in urban environments. *ICAS 2020 Proceedings*. PDF Link
10. Fasano, G., Accardo, D., & Moccia, A. (2016). Sense and avoid for unmanned aircraft systems. *IEEE Aerospace and Electronic Systems Magazine*. IEEE. Article Link
11. Skowron, M., & Chmielowiec, W. (2019). Sense and avoid for small unmanned aircraft systems: Research on methods and best practices. *Proceedings of the 2019 IEEE Radar Conference*. IEEE. Article Link
12. Emshoff, B. L. (2021). Neural Network Classification Approach to Clutter Removal for UTM-Enabling Low-Altitude Radar Surveillance. *OhioLink ETD*. PDF Link
13. Wilson, M. (2012). The use of low-cost mobile radar systems for small UAS sense and avoid. *Sense and Avoid in UAS Research and Applications*. Wiley Online Library. Full Text Link
14. Sahawneh, L. R., Wikle, J. K., & Roberts, A. K. (2018). Ground-based sense-and-avoid system for small unmanned aircraft. *Journal of Aerospace Information Systems*. AIAA. PDF Link
15. Besada, J. A., Campaña, I., Carramiñana, D., & Bergesio, L. (2021). Review and simulation of counter-UAS sensors for unmanned traffic management. *Sensors*, MDPI. PDF Link Hoffer, Keith D., Devin P. Jack, and Tod Lewis. "Terminal Area Considerations for UAS Detect and Avoid." 2019 IEEE/AIAA 38th Digital Avionics Systems Conference (DASC). IEEE, 2019.